

Published in final edited form as:

Neuroimage. 2020 July 15; 215: 116826. doi:10.1016/j.neuroimage.2020.116826.

Gamma oscillations weaken with age in healthy elderly in human EEG

Dinavahi V.P.S. Murty^a, Keerthana Manikandan^a, Wupadrasta Santosh Kumar^a, Ranjini Garani Ramesh^a, Simran Purokayastha^a, Mahendra Javali^b, Naren Prahalada Rao^c, Supratim Ray^{a,*}

^aCentre for Neuroscience, Indian Institute of Science, Bangalore, 560012, India

^bMS Ramaiah Medical College & Memorial Hospital, Bangalore, 560054, India

^cNational Institute of Mental Health and Neurosciences, Bangalore, 560029, India

Abstract

Gamma rhythms (~20–70 Hz) are abnormal in mental disorders such as autism and schizophrenia in humans, and Alzheimer's disease (AD) models in rodents. However, the effect of normal aging on these oscillations is unknown, especially for elderly subjects in whom AD is most prevalent. In a first large-scale (236 subjects; 104 females) electroencephalogram (EEG) study on gamma oscillations in elderly subjects (aged 50–88 years), we presented full-screen visual Cartesian gratings that induced two distinct gamma oscillations (slow: 20–34 Hz and fast: 36–66 Hz). Power decreased with age for gamma, but not alpha (8–12 Hz). Reduction was more salient for fast gamma than slow. Center frequency also decreased with age for both gamma rhythms. The results were independent of microsaccades, pupillary reactivity to stimulus, and variations in power spectral density with age. Steady-state visual evoked potentials (SSVEPs) at 32 Hz also reduced with age. These results are crucial for developing gamma/SSVEP-based biomarkers of cognitive decline in elderly.

Keywords

EEG; Gamma oscillations; Alpha oscillations; SSVEP; Aging; Alzheimer's disease

This is an open access article under the CC BY-NC-ND license (<http://creativecommons.org/licenses/by-nc-nd/4.0/>).

*Corresponding author. sray@iisc.ac.in (S. Ray).

Declaration of competing interest

The authors declare no competing financial interests.

CRedit authorship contribution statement

Dinavahi V.P.S. Murty: Conceptualization, Data curation, Formal analysis, Investigation, Methodology, Visualization, Writing - original draft, Writing - review & editing. **Keerthana Manikandan**: Formal analysis, Data curation, Investigation. **Wupadrasta Santosh Kumar**: Formal analysis. **Ranjini Garani Ramesh**: Data curation, Investigation. **Simran Purokayastha**: Data curation, Investigation. **Mahendra Javali**: Validation, Writing - review & editing. **Naren Prahalada Rao**: Conceptualization, Data curation, Funding acquisition, Methodology, Project administration, Resources, Supervision, Validation, Writing - review & editing. **Supratim Ray**: Conceptualization, Data curation, Formal analysis, Funding acquisition, Methodology, Project administration, Resources, Supervision, Validation, Visualization, Writing - original draft, Writing - review & editing.

1 Introduction

Gamma rhythms are narrow-band oscillations often observed in the electrical activity of the brain, with center frequency occupying ~20–70 Hz frequency range. Previous studies have proposed involvement of these rhythms in certain higher cognitive functions like feature binding (Gray et al., 1989), attention (Chalk et al., 2010; Gregoriou et al., 2009) and working memory (Pesaran et al., 2002). Further, some studies have shown that these rhythms may be abnormal in neuropsychiatric disorders such as schizophrenia (Hirano et al., 2015; Tada et al., 2014), autism (An et al., 2018; Uhlhaas and Singer, 2007; Wilson et al., 2007) and Alzheimer's disease (AD; Mably and Colgin, 2018; Palop and Mucke, 2016).

Gamma rhythms can be induced in the occipital areas by presenting appropriate visual stimuli such as bars and gratings, and their magnitude and center frequency critically depend on the properties of the stimulus such as contrast, size, orientation, spatial frequency and drift rate (Jia et al., 2013; Murty et al., 2018; Ray and Maunsell, 2015). Recently, we showed that large (full-screen) gratings induce two distinct narrow-band gamma oscillations in local field potentials (LFP) in macaque area V1 and posterior electrodes in human EEG, which we termed slow (~20–40 Hz) and fast (~40–70 Hz) gamma (Murty et al., 2018). Fast gamma was not a harmonic of slow, but instead these rhythms were differently tuned to stimulus properties. Importantly, slow gamma was observed only when the grating size was sufficiently large (diameter $>8^\circ$ of visual angle for humans). Two distinct gamma rhythms have also been recently reported in human MEG (Pantazis et al., 2018) and in visual cortex (Veit et al., 2017) and hippocampus (Colgin et al., 2009) in rodents. These rhythms have been suggested to be generated from excitatory-inhibitory interactions of pyramidal cell and interneuron networks (Buzsáki and Wang, 2012), specifically involving parvalbumin and somatostatin interneurons (Cardin et al., 2009; Sohal et al., 2009; Veit et al., 2017).

A recent study has reported parvalbumin interneuron dysfunction in parietal cortex of AD patients and transgenic models of mice (Verret et al., 2012); and aberrant gamma activity in parietal cortex in such mice. However, our knowledge about these rhythms in healthy aging in humans is limited. Studies in human MEG have observed that the center frequency of gamma oscillations is negatively correlated with age of healthy subjects in the range of 8–45 years (Gaetz et al., 2012; Muthukumaraswamy et al., 2010; van Pelt et al., 2018), but our understanding of these rhythms in elderly humans (>49 years), which is clinically more relevant for studying diseases of abnormal aging like AD, is lacking.

Further, visual stimulation of wild type and AD models of mice using light flickering at 40 Hz rescued AD pathology in visual cortex (Iaccarino et al., 2016). Such stimulation is known to entrain brain rhythms and generate steady-state visual evoked potentials (SSVEPs) at 40 Hz. However, to our knowledge, no previous study has examined SSVEPs in gamma band in healthy elderly. Furthermore, a recent study has shown flattening of power spectral density (PSD) in 2–24 Hz range in elderly subjects compared to younger subjects (Voytek et al., 2015). However, how this flattening affects gamma rhythms in elderly has not been examined.

In this study, we described the variation of the two gamma rhythms in healthy elderly subjects. We first used a battery of cognitive tests to identify a large cohort (236 subjects; 104 females) of cognitively healthy elderly subjects aged between 50 and 88 years. For comparison, we also included 47 younger subjects (aged 20–48 years, 16 females). We induced gamma oscillations using full-screen static Cartesian gratings (images consisting of continuous dark and white bars alternating in the x-y plane) while we recorded EEG, and studied how slow and fast gamma and alpha oscillations, as well as slope of the PSD, varied with age in elderly subjects. We also examined SSVEPs in gamma frequency range (32 Hz) in a subset of subjects. As induced gamma band responses were suggested to be affected by microsaccades (Yuval-Greenberg et al., 2008), we monitored subjects' eye movements and microsaccades during analysis. We also examined pupil size, as this is a biological factor that varies physiologically with age (senile miosis) and could affect the overall luminance of the grating by controlling the amount of light incident upon the retina.

2 Materials and methods

2.1 Human subjects

We recruited 236 elderly subjects (104 females) aged 50–88 years from the Tata Longitudinal Study of Aging cohort from urban communities in Bangalore through awareness talks on healthy aging and dementia. Recruitment was done by trained psychologists, who also collected their demographic details. Psychiatrists and neurologists at National Institute of Mental Health and Neurosciences (NIMHANS), Bangalore and M S Ramaiah Hospital, Bangalore assessed the cognitive function of these subjects using a combination of Clinical Dementia Rating scale (CDR), Addenbrook's Cognitive Examination-III (ACE-III), Hindi Mental State Examination (HMSE), and other structured and semistructured interviews. We considered only those subjects who were labelled as cognitively healthy for this study. Out of 236 cognitively healthy subjects thus recruited, we discarded data of 9 subjects (3 females) due to noise (see Artifact Rejection subsection (2.5) below for details). We were thus left with 227 subjects (101 females) aged 50–88 years (mean \pm SD: 66.8 ± 8.2 years) for analysis.

Further, we also recruited 47 younger subjects (16 females) aged 20–48 years (mean \pm SD: 30.4 ± 7.1 years) from the student and staff community of Indian Institute of Science. We screened them orally for any history of neurological/psychiatric illness. We had presented data from 10 of these younger subjects in an earlier study (Murty et al., 2018).

In this study, we have used the words 'gender' and 'sex' interchangeably, denoting biological sex of the subjects. All subjects had reportedly normal or corrected-to-normal vision, although visual acuity was not tested explicitly. They participated in the study voluntarily and against monetary compensation. We obtained informed consent from all subjects for performing the experiment. The Institute Human Ethics Committees of Indian Institute of Science, NIMHANS, Bangalore and M S

Ramaiah Hospital, Bangalore approved all procedures.

2.2 EEG recordings

Experimental setup, EEG recordings and analysis were similar to what we had described in our previous study (Murty et al., 2018). We recorded raw EEG signals from 64 active electrodes (actiCAP) using BrainAmp DC EEG acquisition system (Brain Products GmbH). We placed the electrodes according to the international 10-10 system. We filtered raw signals online between 0.016 Hz (first-order filter) and 1000 Hz (fifth-order Butterworth filter), sampled at 2500 Hz and digitized at 16-bit resolution (0.1 μ V/bit). We rejected electrodes whose impedance was more than 25 K Ω . This led to a rejection of 3.9% of electrodes in elderly age-group (1.1% in younger subjects). However, most of these electrodes were frontal/central, and specifically, none were the ten parieto-occipital/occipital electrodes used for analyses (see Data Analysis subsection (2.6)). Impedance of the final set of electrodes was 5.5 ± 4.2 K Ω (mean \pm SD) for elderly subjects and 3.7 ± 3.4 K Ω for younger subjects. We referenced EEG signals to FCz during acquisition (unipolar reference scheme).

2.3 Experimental setting and behavioral task

All subjects sat in a dark room in front of an LCD screen with their head supported by a chin rest. The screen (BenQ XL2411) had a resolution of 1280×720 pixels and a refresh rate of 100 Hz. It was gamma-corrected and was placed at a mean \pm SD distance of 58.1 ± 0.9 cm from the subjects (53.9–63.0 cm for all 274 subjects, 54.9–61.0 cm for the 227 elderly subjects) according to their convenience (thus subtending a width of at least 52° and height of at least 30° of visual field for fullscreen gratings). We calibrated the stimuli to the viewing distance in all cases.

Subjects performed a visual fixation task. Stimulus presentation was done by a custom software running on MAC OS that also controlled the task flow. Every trial started with the onset of a fixation spot (0.1°) shown at the center of the screen, on which the subjects were instructed to hold and maintain fixation. After an initial blank period of 1000 ms, a series of stimuli (2–3) were randomly shown for 800 ms each with an interstimulus interval of 700 ms. Stimuli were sinusoidal luminance gratings presented full screen at full contrast. For the main “Gamma” experiment, these were presented at one of three spatial frequencies (SFs): 1, 2, and 4 cycles per degree (cpd) and one of four orientations: 0° , 45° , 90° and 135° . We chose these stimulus parameters as these were shown to induce robust gamma previously (Murty et al., 2018). Stimuli were presented in pseudorandom order to prevent adaptation effects. Subjects performed this task during a single session that lasted for ~ 20 min, divided in 2–3 blocks with 3–5 min breaks in between, according to their comfort (total 597 blocks across 283 subjects). For an initial subset of subjects, stimuli with SF of 0.5 and/or 8 were also presented, but we discarded these SFs from further analysis to maintain uniformity. We also tested 32-Hz SSVEPs on a subset of the subjects who had analyzable data for the Gamma experiment (221/227 elderly and 46/47 younger subjects) according to their willingness. One grating with a single SF and orientation that showed highest change in slow and fast gamma power was chosen from the Gamma experiment for each subject, after preliminary analysis done during the recording session (as explained in Data Analysis subsection (2.6) below). This grating was randomly presented in a trial either as a static grating or phase-reversal grating that counter-phased at 16 cycles per second (cps) in a

similar stimulus presentation paradigm as the Gamma experiment (2–3 stimuli per trial, stimulus period: 800 ms, interstimulus interval: 700 ms). We chose 16 cps for two reasons. First, in a different study in which we recorded the responses of spikes and local field potentials (LFP) obtained using microelectrode arrays implanted in the primary visual cortex of awake monkeys, we found that the SSVEP gain was highest between 12 and 16 cps (Salelkar and Ray, 2020). Second, gratings counter-phasing at 16 Hz produced SSVEP responses at 32 Hz, i.e. twice the counter-phasing frequency (as shown in Fig. 8), which was between the two gamma bands of interest. Subjects performed this experiment for 3–5 min during the same session as the Gamma experiment. We presented each stimulus ~30–40 times for both the Gamma and SSVEP experiments according to the subjects' comfort and willingness. Unless otherwise stated, stimulus presentation of a particular orientation and spatial frequency is referred to as a “stimulus repeat” in this paper.

2.4 Eye position analysis

We recorded eye signals (pupil position and diameter data) using EyeLink 1000 (SR Research Ltd., sampled at 500 Hz) during the entire trial for all but one subject. We calibrated the eye-tracker for pupil position and monitor distance for each subject before the start of the session. All the subjects were able to maintain fixation with a standard deviation of less than 0.6° (elderly, eye-data for Gamma experiment shown in Fig. 7a) and 0.4° (young, data not shown). We defined fixation breaks as eye-blinks or shifts in eye-position outside a square window of width 5° centered on the fixation spot. We rejected stimulus repeats with fixation breaks during -0.5s – 0.75s of stimulus onset, either online (and repeated the stimulus thus discarded), or offline (we took a few additional trials to compensate for possible offline rejection), according to the subjects' comfort. This led to rejection of $16.7 \pm 14.2\%$ (mean \pm SD) and $16.7 \pm 15.1\%$ stimulus repeats (for Gamma and SSVEP experiments respectively) for elderly subjects (most of them preferred offline rejection). For younger subjects, for many of whom we used online eyemonitoring, the rate of rejection due to fixation breaks was low ($4.9 \pm 5.7\%$ and $4.2 \pm 7.0\%$).

2.5 Artifact rejection

We first estimated bad stimulus repeats for each unipolar electrode separately as described next. We applied a trial-wise thresholding process on both raw waveforms (high-pass filtered at 1.6 Hz to eliminate slow trends if any) and multi-tapered PSD (computed between -500 ms and 750 ms of stimulus onset using Chronux toolbox (Mitra and Bokil, 2008, <http://chronux.org/>, RRID:SCR_005547)). Any stimulus repeat for which either the waveform or PSD deviated by 6 times the standard deviation from the mean at any time bin (between -500 ms and 750 ms) or frequency point (between 0 and 200 Hz) was considered a bad repeat for that electrode. We then created a common set of bad repeats across all 64 unipolar electrodes by first discarding those electrodes that had more than 30% of all repeats marked as bad, and subsequently assigning any repeat as bad if it occurred in more than 10% of total number of remaining electrodes. Finally, any repeat that was marked bad in any of the ten unipolar electrodes used for analysis (P3, P1, P2, P4, PO3, POz, PO4, O1, Oz, and O2; see Data Analysis subsection (2.6)) was unconditionally included in the common bad repeats list, providing a final list of common bad repeats for each block for each subject. In spite of

these stringent conditions, these led to a rejection of less than 20% of data ($18.4 \pm 6.4\%$ and $17.0 \pm 5.1\%$ for elderly and younger subjects).

In addition, we calculated slopes (see Data Analysis subsection (2.6)) of PSD (calculated with 1 taper and averaged across repeats, after removal of bad repeats) for each block in 56 Hz–84 Hz range (to include the fast gamma range) for each unipolar electrode. Previous studies have shown that in clean electrophysiological data, PSD slopes are typically between 0.5 and 4.5 (Muthukumaraswamy and Liley, 2018; Podvalny et al., 2015; Sheehan et al., 2018; Shirhatti et al., 2016). We therefore discarded those electrodes ($5.0 \pm 5.9\%$ for elderly and $5.2 \pm 7.7\%$ for younger subjects) that had PSD slopes less than 0. We further discarded any block (53/497 and 5/100 for elderly and younger subjects) that did not have at least a single clean bipolar electrode pair in any of the three groups of bipolar electrodes used for analysis (depicted in Fig. 3d, see Data Analysis subsection (2.6) for details): PO3–P1, PO3–P3, POz-PO3 (left anterolateral group); PO4–P2, PO4–P4, POz-PO4 (right anterolateral group) and Oz-POz, Oz-O1, Oz-O2 (posteromedial group). We then pooled data across all good blocks for every subject separately for final analysis. Those subjects who did not have any analyzable blocks (9/236 and 0/47 for elderly and younger subjects respectively) were discarded from further analysis, leaving 227 elderly (aged 50–88 years, mean \pm SD: 66.8 ± 8.2 years, females: 101) and 47 young subjects (aged 20–48 years, mean \pm SD: 30.4 ± 7.1 years, females: 16) for analysis. The total number of repeats per electrode that were finally analyzed were 276.2 ± 87.2 for elderly subjects and 270.4 ± 67.4 for younger subjects.

We applied a similar artifact rejection procedure for SSVEP experiment. Out of subjects with analyzable blocks for the Gamma experiment, 197 elderly (mean \pm SD: 66.8 ± 7.8 years, females: 93) and 43 young subjects (mean \pm SD: 30.4 ± 7.3 years, females: 15) had analyzable blocks (242/270) for SSVEP experiment. Using similar selection criteria as before, we rejected $7.7 \pm 5.2\%$ of repeats for elderly subjects and $6.6 \pm 4.1\%$ for younger subjects. The total number of analyzed repeats per electrode for counter-phasing condition were 30.2 ± 6.9 and 29.7 ± 6.6 for elderly and younger subjects respectively.

2.6 EEG data analysis

Our primary emphasis was to characterize gamma and other spectral signatures as a function of age within the elderly population (>49 years), for which we divided these subjects into two groups: 50–64 years (95 subjects; 51 females) and >64 years (141 subjects, 53 females). For completeness, we also show results from a cohort of younger subjects aged between 20 and 49 years (47 subjects; 16 females).

In this study, we wanted to employ methods that can be easily and readily employed for screening larger populations of patients. Hence, we used electrode-level (sensor-level) analyses instead of source space, for which the results depend on the availability of structural MRI data as well as the details of the source localization technique. For all analyses (unless otherwise mentioned), we used bipolar reference scheme. We rereferenced data at each electrode offline to its neighboring electrodes. We thus obtained 112 bipolar pairs out of 64 unipolar electrodes (Murty et al., 2018, depicted in Fig. 3e). We considered the following bipolar combinations for analysis, except for scalp maps: PO3–P1, PO3–P3, POz-PO3 (left anterolateral group); PO4–P2, PO4–P4, POz-PO4 (right anterolateral group)

and Oz-POz, Oz-O1, Oz-O2 (posteromedial group), depicted in Fig. 3d. We discarded a bipolar electrode if either of its constituting unipolar electrodes was marked bad as described in the previous subsection (2.5). Data was pooled for the rest of the bipolar combinations in each of the electrode groups for further analysis.

We analyzed all data using custom codes written in MATLAB (The MathWorks, Inc, RRID:SCR_001622). We computed PSD and the time-frequency power spectrograms using multi-taper method with a single taper using Chronux toolbox. We chose baseline period between -500 ms and 0 ms of stimulus onset, while stimulus period between 250 ms and 750 ms to avoid stimulus-onset related transients, yielding a frequency resolution of 2 Hz for the PSDs. We calculated time frequency power spectra using a moving window of size 250 ms and step size of 25 ms, giving a frequency resolution of 4 Hz.

We calculated change in power in alpha rhythm and the two gamma rhythms as follows:

$$\Delta Power = 10 \left(\log_{10} \frac{\sum_f ST(f)}{\sum_f BL(f)} \right)$$

Where ST and BL are stimulus and baseline power spectra (across frequency f) averaged across repeats for all stimulus conditions and analyzable bipolar electrodes. For alpha, $f \in [8, 12]$ Hz, for slow gamma, $f \in [20, 34]$ Hz and for fast gamma, $f \in [36, 66]$ Hz. We estimated baseline absolute power (or power in baseline period) as $\log_{10}(\text{mean}(BL(f)))$: We defined the center frequency for a gamma rhythm as the frequency at which the change in power (in these averaged PSDs) was maximum within that gamma range.

Note that even though we presented stimuli of 12 different conditions (combinations of 3 SFs and 4 orientations), we pooled across these conditions instead of analyzing these separately, because the primary motive of the current study was to study the variation of gamma with age and not stimulus characteristics (which we addressed in Murty et al., 2018). This yielded more than 250 stimulus repeats on average per subject for final analysis. For SSVEP experiment, we analyzed only the counter-phasing gratings and took the power at 32 Hz (twice the counter-phasing frequency, i.e. 16 cps) for analysis. The static gratings that were presented mainly to prevent adaptation were discarded.

We generated scalp maps using the `topoplot.m` function of EEGLAB toolbox (Delorme and Makeig, 2004, RRID:SCR_007292), modified to show each electrode as a colored disc, with color representing the change in power of slow gamma/fast gamma/SSVEP from baseline in decibels (dB).

We calculated slopes for rejecting noisy electrodes (as described in (2.5)) by fitting PSD across all analyzable repeats for each individual unipolar electrode with a power-law function as $P(f) = A \cdot f^\beta$, where P is the PSD across frequencies $f \in [56, 84]$ Hz. A (scaling factor) and β (slope) are free parameters obtained using least square minimization using the program `fminsearch` in MATLAB. We similarly estimated slopes for PSDs averaged across analyzable unipolar or bipolar electrodes during baseline period (-0.5 to 0 ms) for Supplementary Fig. 2.

2.7 Microsaccades and pupil data analysis

We detected microsaccades using a threshold-based method described earlier (Murty et al., 2018), initially proposed by (Engbert, 2006). In brief, we categorized eye movements with velocities that crossed a specified threshold for at least a specified duration of time as microsaccades. We set the velocity threshold between 3 and 6 times the standard deviation of eye-velocities and minimum microsaccade duration between 10 and 15 ms for every subject so as to maximize the correlation between peak velocity and amplitude of all microsaccades for that subject (also called a “main sequence”, see Engbert, 2006 for details), while maintaining the minimum microsaccade velocity at 10°/s and the microsaccade rate between 0.5/s and 3.0/s.

The above algorithm was applied for the analysis period of -0.5 s to 0.75 s of stimulus onset. After removing the microsaccade-containing repeats, there were 128.1 ± 71.1 (mean \pm SD, minimum 5) repeats for elderly subjects ($n = 226$, excluding 1 subject for whom eye-data could not be collected) for anterolateral electrodes reported in Fig. 7c. Results did not change when we discarded 13 elderly subjects with less than 30 repeats without microsaccades from analysis (data not shown).

EyeLink 1000 system recorded pupil data in arbitrary units for every subject since pupil data cannot be calibrated for this tracker. Hence, instead of directly comparing time-series of pupil data, we used coefficient of variation (CV, ratio of standard deviation to mean) for every repeat as a measure of pupillary reactivity to stimulus of that repeat. This simple measure scales standard deviation of a distribution with respect to its mean. This allows comparison of variation in different distributions without getting affected by the mean of the distributions. We calculated CV for each analyzable trial separately and calculated mean CV across trials for every subject for comparison.

2.8 Statistical analysis

Our findings were based mainly on PSD plots and we used appropriate statistical methods (Pearson correlation, linear regression and ANOVA) to confirm our interpretations. We used one-way (or two-way, as necessary) ANOVA to compare means of bar plots in Fig. 4c, d, 6a and 8c, although non-parametric tests on medians instead of means using Kruskal-Wallis test (not reported) yielded qualitatively similar results. For two-way ANOVA, we considered age-group and sex as independent factors although including their interaction effect in the model yielded qualitatively similar results (not reported). We used Bonferroni correction for multiple tests/comparisons wherever necessary.

2.9 Data and code availability

The EEG data presented here is recorded as part of a large multiinvestigator project that involved several other experiments and measurements like psychophysics, fMRI, PET, etc., some of which are still in progress. Hence, the data would be made publicly available at a later time according to the policies of the project. All spectral analyses were performed using Chronux toolbox (version 2.10), available at <http://chronux.org>.

3 Results

We recorded EEG from 236 elderly subjects aged 50–88 years and 47 subjects aged 20–48 years while presenting full-screen sinusoidal grating stimuli on a computer monitor (see subsections 2.1 and 2.3 of Materials and Methods for details). Fig. 1 shows the results of an example subject, a 53 years old female. Trial-averaged evoked potentials were plotted for electrodes P3, P1, P2, P4, PO3, POz, PO4, O1, Oz, O2 for unipolar reference (Fig. 1a, left column) and PO3–P1, PO3–P3, POz–PO3, PO4–P2, PO4–P4, POz–PO4, Oz–POz, Oz–O1 and Oz–O2 for bipolar reference (Fig. 1a, right column). The bipolar channels are shown as dots in scalp maps in Fig. 1c. These traces revealed a transient in the first 250 ms of stimulus onset and after the stimulus offset (i.e. after 800 ms). For the same set of electrodes, trial-wise power spectrograms were averaged to generate raw spectrogram and change in power spectrogram (w.r.t. a baseline period of –500 ms to 0 ms of stimulus onset). Although not noticeable in the evoked potential traces and raw spectrograms, these stimuli elicited prominent gamma band responses as seen in the change in power spectrograms. These responses were in slow gamma (~20–34 Hz) and fast gamma (~36–66 Hz) range. Consistent with previous results (Murty et al., 2018), these responses were seen during the stimulus period (after the onset-transient) and were best noticed for bipolar reference as compared to unipolar reference. Also, slow gamma power showed a gradual build-up whereas fast gamma power showed a decreasing trend with stimulus duration (Fig. 1a, bottom row). Alpha (8–12 Hz) power suppression was very weak in this subject. We also plotted power spectral densities (PSD) in the baseline period (dotted black trace in Fig. 1b) and stimulus period (250 ms–750 ms; solid black trace in Fig. 1b) and change in power spectrum (blue trace in Fig. 1b). Prominent ‘bumps’ in the slow and fast gamma range were noticeable in PSD in the stimulus period as well as change in spectrum. Also, no ‘bump’ was noticeable in the baseline PSD in the alpha range for this subject. These changes were most prominent in the parieto-occipital and occipital electrodes, as seen in the scalp maps for the bipolar reference case in Fig. 1c.

3.1 Baseline absolute power of slow and fast gamma, broadband myogenic activity and slopes of baseline PSDs did not differ across the elderly age-groups

A recent study (Voytek et al., 2015) has suggested that PSDs of elderly subjects seem to be “rotated” around 15 Hz, with less power at frequencies lower than ~15 Hz and more power at higher frequencies, as compared to younger subjects. This rotation of PSDs with age could lead to flatter PSDs in elderly subjects and could potentially bias the estimation of change in power in slow and fast gamma range in subjects of different age groups. This is because higher baseline absolute power in these rhythms in older subjects may lead to lower estimates of change in power. Hence, we first checked whether there was any difference in baseline PSDs across age. We calculated mean baseline PSDs of 10 unipolar electrodes and 9 bipolar electrodes separately, as mentioned above. We compared PSDs between 2 and 200 Hz in two elderly groups (50–64 years and >64 years groups) as well as the younger group (20–49 years; Fig. 2a and b for males and females), and males versus females (averaged across all ages; Fig. 2c).

Because our primary emphasis was on comparison within the elderly group, we first compared the PSDs between the two elderly subgroups (dark and light gray traces in Fig. 2a and b). The PSDs indeed appeared to become flatter with age (light gray trace was above the dark gray trace), but this effect was prominent only at frequencies above ~50 Hz. In the slow and fast gamma ranges (indicated by colored bars on the abscissa of plots in Fig. 2), the two gray traces were largely overlapping. To quantify this, we performed a two-way ANOVA on baseline absolute powers of alpha, slow gamma and fast gamma (averaged across frequencies for each band) with age-group (50–64 or >64 years) and sex as factors and found that effect of age group was not significant for power in any band ($p > 0.05$ in all cases except for fast gamma in the bipolar case where $p = 0.03$, which was not significant at Bonferroni corrected significance level of $0.05/3 = 0.016$). Results were not qualitatively different when we performed one-way ANOVA for baseline absolute power of alpha/slow/fast gamma across age-groups for males and females separately ($p > 0.05$ for all cases except for fast gamma in females for bipolar case where $p = 0.03$).

We obtained similar trends for comparisons (one-way ANOVA separately for males and females) between younger (<50 years) and elderly subjects (50 years and above). Baseline absolute powers in alpha/slow/fast gamma ranges were not significantly different for younger and elderly male subjects in either reference schemes (Fig. 2a, $p > 0.05$ for all cases). However, elderly females had more baseline fast gamma power compared to younger females ($F(1,115) = 7.9$, $p = 0.006$) in bipolar case and lesser alpha power in both unipolar ($F(1,115) = 17.6$, $p = 5.5 \times 10^{-5}$) and bipolar ($F(1,115) = 6.5$, $p = 0.012$) cases (Fig. 2b). These differences could be due to a small sample size of females in the younger age-group ($n = 16$).

Across genders, females had significantly higher baseline slow gamma power than males (Fig. 2c, data pooled across all 274 subjects; one-way ANOVA across gender: $F(1,272) = 24.5/27.9$, $p = 1.3 \times 10^{-6}/2.6 \times 10^{-7}$ for unipolar/bipolar reference schemes) and higher alpha power ($F(1,272) = 4.6/8.4$, $p = 0.03/0.004$ for unipolar/bipolar conditions). However, baseline fast gamma power was not significantly different ($p > 0.05$ for both reference schemes). Amongst the elderly subjects ($n = 227$, data not shown), females had only higher slow gamma compared to males ($F(1,225) = 16.4/21.3$, $p = 7.1 \times 10^{-5}/6.4 \times 10^{-6}$ for unipolar/bipolar conditions for slow gamma, $F(1,225) = 5.3$, $p = 0.022$ for alpha in bipolar case and $p > 0.05$ for all other cases).

We next checked if there was any increased myogenic activity in elderly subjects due to factors like physical strain during the session. Stronger myogenic artefacts in these subjects could increase noise floor and decrease probability of detection of the gamma peaks. Whitham et al. (2008) suggested that myogenic activity affects higher frequencies (30–100 Hz) in PSDs of electrodes located more peripherally than towards the center. We calculated baseline broadband power averaged across 30–100 Hz (excluding 50 Hz and 100 Hz peaks that represented line noise and monitor refresh rate) across all unipolar (Supplementary Fig. 1a, left column) and bipolar electrodes (Supplementary Fig. 1b, left column, plotted across three age-groups for males and females separately). We noticed that baseline broadband power was comparable for most electrodes across the three age-groups. We quantified this by performing one-way ANOVA on baseline absolute power at each electrode across the

three age-groups (Supplementary Figs. 1a and 1b, right column). We found very few electrodes that showed a significance level of 0.01 or less, for both unipolar and bipolar cases. Thus, we ruled out the possibility that elderly subjects had more myogenic activity in their EEG data than the younger subjects.

To test for the rotation of PSDs with age as suggested by Voytek et al. (2015), we computed the slopes between 16 and 44 Hz (Supplementary Fig. 2; see Data analysis subsection (2.6) for details; this range was chosen to avoid the bump in the alpha band at the lower end and the 50 Hz noise at the higher end). Two-way ANOVA with age (young and elderly) and sex (male and female) as factors showed no significant difference in the slopes between young and elderly subjects for either unipolar or bipolar reference scheme case ($p > 0.05$). However, females had steeper slopes compared to males ($F(1,271) = 7.9$, $p = 0.005$ and $F(1, 271) = 31.4$, $p = 5.1 \times 10^{-8}$ for unipolar and bipolar cases respectively, Supplementary Fig. 2a). Since females had higher baseline alpha power compared to males (Fig. 2c), we tested whether any differences in baseline PSD slopes could be because of differences in baseline alpha power. We divided baseline PSDs of all subjects (young and elderly pooled together) into terciles based on alpha power (Fig. 2d). Subjects who had higher baseline alpha power also had steeper PSD slopes. Regression of PSD slopes in 16–44 Hz frequency range with baseline alpha power was significant for both reference schemes (Supplementary Fig. 2b). Further, when we performed partial correlation of slopes with age and baseline alpha power, slopes were significantly correlated with alpha power ($\rho = 0.57$, $p = 5.4 \times 10^{-25}$ and $\rho = 0.58$, $p = 3.1 \times 10^{-26}$ for unipolar and bipolar cases respectively) but not with age ($\rho = 0.07$ and -0.12 for unipolar and bipolar, $p > 0.05$ for both). Thus, PSD slope was not influenced by age, but by baseline alpha power. We discuss these results in the context of the findings of Voytek and colleagues in the Discussion.

3.2 Gamma was observed in more than 80% of subjects

As reported in our earlier study (Murty et al., 2018) and as in Fig. 1, gamma was best observed, as a response to full-screen 100% contrast Cartesian visual gratings, in bipolar referencing scheme compared to unipolar. Hence, we limited further analysis to bipolar referencing. We divided the 9 bipolar electrodes mentioned above into 3 groups (Fig. 3d): PO3–P1, PO3–P3, POz-PO3 (left anterolateral group); PO4–P2, PO4–P4, POz-PO4 (right anterolateral group) and Oz-POz, Oz-O1, Oz-O2 (posteromedial group). For each subject, we chose the electrode group that had maximum change in power in slow and fast gamma ranges added together. We labelled a subject as having either of the gamma rhythms if the change in power in these rhythms during stimulus period (calculated from data pooled across electrodes chosen for the subject) exceeded an arbitrarily chosen threshold of 0.5 dB from baseline. Fig. 3a shows scatter plot of slow versus fast gamma change in power for all subjects. Based on our threshold, ~84% of subjects had at least one gamma (slow: ~77% and fast: ~64%), while ~57% of subjects had both the gammas, which could be observed as distinct “bumps” in the change in PSD from baseline (Fig. 3b). Fig. 3c shows the percentage of subjects in each age-group who had no/slow/fast/both gammas based on our threshold. The percentage of subjects who had only fast gamma or both gammas was highest in 20–49 years age-group and lowest in >64 years age-group.

Fig. 3e shows change in power in slow (top row) and fast (bottom row) gamma rhythms across all electrodes (plotted as disks) for the young (left column) and the two elderly age-groups (middle and right columns). Both gamma rhythms were best observed in the same 9 bipolar electrodes mentioned above and depicted in Fig. 3d and e. Further, power in both gamma bands appeared to decrease with age across the two elderly age-groups, although the results were more prominent for fast gamma.

3.3 Change in gamma power was negatively correlated with age

To quantify this difference, we tested how gamma oscillations correlated with age in these electrode groups. We tested for anterolateral and posteromedial groups separately (Fig. 4 and Supplementary Fig. 3 respectively). For Fig. 4, out of the left and right anterolateral groups, we chose that group which had maximum slow and fast gamma power change summed together. Figs. 4a and b show mean change in spectrograms and PSDs respectively for the three age-groups separately for males and females. These plots highlight all the major results discussed later. First, both slow and fast gamma power reduced with age. This was observed between young and elderly groups (black versus the other two traces), and also within the two elderly sub-groups (dark and light gray traces). Second, peak frequencies of both slow and fast gamma reduced with age. Third, alpha suppression (change in 8–12 Hz power from baseline) in the stimulus period was more pronounced in young versus elderly, but there was no difference between the two elderly sub-groups.

The first observation was also reflected in the gamma power computed within the pre-specified ranges (as shown in the bar plots shown in Fig. 4c and d), but there were some caveats. We computed the total power within a pre-specified band by simply summing the absolute power values within the band, which typically has larger contribution from lower frequencies because the absolute power is larger compared to that in higher frequencies within the band. This is not reflected in Fig. 4b because it only shows the change in power with respect to the baseline period. Consequently, if the traces are overlapping at lower frequencies within the band and diverge at higher frequencies, which was the case in the slow gamma range for both males and females (Fig. 4b), the total power in the band may not be significantly different. In particular, for young females, the power at the start of the slow gamma band (20–26 Hz) was slightly lower than the elderly subgroups (Fig. 4b, bottom plot, black versus gray traces), but became higher at higher frequencies within the slow gamma band (28–34 Hz). However, because the absolute power is higher between 20 and 26 Hz than 28–34 Hz, the total slow gamma power was actually lower for young females compared to elderly (Fig. 4c, black versus gray bars). These issues can be partially addressed by changing the frequency range over which gamma is computed (dependent on age and potentially even across subjects), but then the results are dependent on the level of customization of ranges, which we wanted to minimize. We observed that younger subjects had significantly more fast but not slow gamma than elderly subjects (two-way ANOVA with age-group (20–49 and > 49 years) and sex as factors, $F(1,271) = 1.3/35.6$, $p = 0.2/7.6 \times 10^{-9}$ for slow/fast gamma across age-groups). Also, females had more slow and fast gamma than males (same two-way ANOVA, $F(1,271) = 4.7/37.9$, $p = 0.03/2.5 \times 10^{-9}$ for slow/fast gamma).

Among the elderly subjects, visual inspection of change in spectrograms and spectra revealed that both slow and fast gamma power was less in subjects of >64 years age-group compared to 50–64 years age-group. This trend was also noticeable in the bar plots in Fig. 4c and d for both genders. As before, it was significant only for fast gamma (two-way ANOVA with age-group (50–64 and > 64 years) and gender as factors; $F(1,224) = 2.4/11.4$, $p = 0.12/8.4 \times 10^{-4}$ for slow/fast gamma across age-group). Females had higher slow and fast gamma compared to males (same two-way ANOVA, $F(1,224) = 7.4/21.7$, $p = 0.007/5.4 \times 10^{-6}$ for slow/fast gamma across gender). We further quantified this observation by regressing change in slow and fast gamma power across age (scatter plots in Fig. 4c and d). When the regression was done separately for males and females, the slopes were always negative (males: $\beta = -0.008/-0.018$ and females: $\beta = -0.018/-0.016$ for slow/fast gamma) but did not reach significance except for fast gamma in elderly males ($p = 2.4 \times 10^{-4}$). When we pooled data across both genders, the results were significant (linear regression, $\beta = -0.02$, $R^2 = 0.02$, $p = 0.022$ and $\beta = -0.02$, $R^2 = 0.08$, $p = 1.4 \times 10^{-5}$ for slow and fast gamma respectively). These trends did not differ when we included power in baseline period in the linear regression model ($\beta_{\text{Age}} = -0.017$, $\beta_{\text{BaselinePower}} = 0.024$, $R^2 = 0.02$, $p = 0.021$ for slow gamma and $\beta_{\text{Age}} = -0.022$, $\beta_{\text{BaselinePower}} = -0.11$, $R^2 = 0.08$, $p = 1.4 \times 10^{-5}$ for fast gamma). Partial correlation of stimulus-induced change in power with age and baseline absolute power indicated that the effect of age on change in power was significant ($\rho = -0.15$, $p = 0.02$ and $\rho = -0.27$, $p = 2.9 \times 10^{-5}$ for slow and fast gamma respectively) but not the effect of baseline power ($p > 0.05$ for both gamma). Similar, albeit weaker results were observed in the posteromedial group of electrodes for slow gamma (Supplementary Fig. 3c; linear regression, $\beta = -0.016$, $R^2 = 0.02$, $p = 0.04$) as well as fast gamma (Supplementary Fig. 3d; $\beta = -0.02$, $R^2 = 0.04$, $p = 0.001$).

3.4 Center frequency of slow and fast gamma was negatively correlated with age

Gamma peak center frequency was shown to decrease with age in an age group between 8 and 45 years (Gaetz et al., 2012; Muthukumaraswamy et al., 2010). This was observed in our data as well as noted above. To examine the change in center frequency of slow and fast gamma rhythms in elderly in more detail, we plotted the change in power spectra (frequencies mentioned on abscissa) vs age (on ordinate, arranged in increasing order from top to bottom) of all 227 elderly subjects, separately for anterolateral (left column) and posteromedial (right column) group of electrodes (Supplementary Fig. 4a). We defined center frequency for each gamma as the frequency that had maximum change in power in the frequency range of that gamma, provided the total change in power in that gamma band was greater than our threshold of 0.5 dB (represented by circles and triangles for slow and fast gamma in Supplementary Fig. 4a; number of subjects having slow and fast gamma power change above this threshold is mentioned in Fig. 5). Fig. 5 shows the same result as scatter plots of center frequencies of slow (left column) and fast gamma (right column) plotted against the age of the subjects for anterolateral group of electrodes. Solid line in Fig. 5 indicates regression fit of center frequencies against age, showing a decreasing trend which was significant for both slow and fast gamma (linear regression for center frequency vs age: $\beta = -0.08$, $R^2 = 0.04$, $p = 0.008$ for slow gamma and $\beta = -0.16$, $R^2 = 0.06$, $p = 0.008$ for fast gamma). Similar, albeit weaker results were observed for the posteromedial group (Supplementary Fig. 4b; fast gamma: $\beta = -0.17$, $R^2 = 0.06$, $p = 0.008$; slow gamma: $\beta =$

-0.06 , $R^2 = 0.02$, $p = 0.052$). Note that because our analysis was done over 500 ms of data, the frequency resolution was 2 Hz, which limited our ability to observe small shifts in the peak frequency.

3.5 Frequency of peak alpha suppression reduced with age in elderly subjects, but not change in alpha power

We noticed prominent alpha suppression for younger as well as elderly subjects, as noted above. Alpha suppression was stronger in younger subjects compared to elderly subjects (data for anterolateral group is shown in Fig. 6a; two-way ANOVA with age-groups (20–49 and >49 years) and gender as factors; $F(1,271) = 33.2$, $p = 2.2 \times 10^{-8}$ across age-groups), but did not differ significantly between genders ($F(1,271) = 0.5$, $p = 0.49$ across gender). To rule out the potential contribution of baseline absolute alpha power to these results, we performed two-way ANOVA of alpha suppression with age-groups as a categorical variable and baseline absolute alpha power as a continuous variable. While baseline absolute power proved to be a significant factor as expected ($F(1,271) = 49.5$, $p = 1.6 \times 10^{-11}$), we found that age-group (younger or elderly) also had a significant effect on alpha suppression ($F(1,271) = 27.7$, $p = 2.8 \times 10^{-7}$).

Amongst elderly subjects however, alpha suppression did not differ across age-groups (50–64 and >64 years) and gender (two-way ANOVA, $p > 0.05$ for both age-group and gender). We further confirmed this observation by regressing alpha suppression across age for all the elderly subjects (scatter plot in Fig. 6a). Alpha suppression was not significantly correlated with age for either gender or for data pooled across genders ($p > 0.05$ for all cases). Performing partial correlation of alpha suppression with age and baseline absolute power did not improve the trends we described above for age. Finally, the trends were not qualitatively different when we repeated the analysis for the posteromedial group of electrodes. This is also observed in the scalp maps shown in Fig. 6b.

Finally, we tested for frequency of peak alpha suppression in the elderly, since previous studies have shown that alpha peak frequency reduces with age (see for example, Ishii et al., 2017; Kropotov, 2016; and Fig. 1 of Sahoo et al., 2020). We interpret our results with caution because we were left out with only 3 frequency points in the alpha range (8, 10 and 12 Hz) due to the limited frequency resolution (2 Hz) of our PSDs. We limited the analysis to subjects for whom the alpha suppression was 0.5 dB or more ($N = 45$ for 50–64 years age group, $N = 58$ for >64 years), as done for gamma analysis above. We found that frequency of peak alpha suppression in anterolateral electrodes was significantly smaller in >64 years age-group (mean \pm SEM: 10.38 ± 0.12 Hz, $N = 58$) compared to 50–64 years age-group (mean \pm SEM: 10.98 ± 0.10 Hz, $N = 45$). One-way ANOVA revealed significant effect of age-group on frequency of peak alpha suppression ($F(1,101) = 5.7$, $p = 0.02$, data not shown). Trends were qualitatively similar for posteromedial group of electrodes. Therefore, in spite of the poor frequency resolution, we found significant reduction in alpha peak frequency with age, consistent with previous studies.

Microsaccades and pupillary reactivity did not contribute to negative correlation between change in gamma power and age

Next, we studied the potential contribution of eye-movement (including microsaccades) and pupillary diameter on our results. Fig. 7a shows mean eye-position for each of the elderly age-groups in horizontal (top row) and vertical (middle row) directions ($n = 226$, eye data was unavailable in one subject; thickness represents SEM). Eye position did not vary in the two age-groups in either direction. Further, we extracted microsaccades for every analyzed trial for every subject in the two age-groups (see subsection 2.7 of Materials and Methods). The two groups had comparable microsaccade rates ($0.80 \pm 0.05/s$ and $0.88 \pm 0.05/s$). Fig. 7b shows a scatter plot of peak velocity versus maximum displacement for each microsaccade (a plot called “main sequence”, see Engbert, 2006). These microsaccade clouds were highly overlapping for these two groups. Histograms of microsaccade rate during $-0.5 - 0.75$ s of stimulus onset for both the elderly age-groups were also highly overlapping (Fig. 7a, bottom row), although we see a trend of slightly higher microsaccade rate for subjects aged >64 years compared to 50–64 years age-group. We then computed power after removing trials containing microsaccades (see subsection 2.7 of Materials and Methods for details), and could replicate the results in Fig. 4: change in both slow and fast gamma power decreased with age significantly ($\beta = -0.02$, $R^2 = 0.03$, $p = 0.015$ for slow gamma and $\beta = -0.02$, $R^2 = 0.08$, $p = 2.7 \times 10^{-5}$ for fast gamma, Fig. 7c).

We next tested if pupillary reactivity to stimulus presentation affected change in gamma power with age. We calculated mean coefficient of variation (CV) of pupil diameter across every analyzable trial for all 226 subjects (eye data was unavailable in one subject). We observed that mean CV decreased significantly with age in the elderly subjects, possibly because of senile miosis (Pearson correlation, $r = -0.24$, $p = 3.5 \times 10^{-4}$, Fig. 7d top row). However, neither slow nor fast gamma power varied with mean CV of pupil diameter (slow/fast: $r = 0.07/0.1$, $p = 0.31/0.14$ and $r = 0.09/0.12$, $p = 0.19/0.06$ for anterolateral (Fig. 7d middle and bottom rows) and posteromedial electrodes respectively (data not shown)).

3.7 SSVEP power at 32 Hz was negatively correlated with age

Finally, we checked whether SSVEPs in the gamma range were affected by healthy aging. Specifically, we tested 32-Hz SSVEPs elicited by gratings counter-phasing at 16 cps. Figs. 8a and b show change in power spectrograms and spectra respectively for males and females separately for the two elderly and the younger age-groups for the anterolateral group of electrodes, with same conventions as in Fig. 4. We saw clear peaks at 32 Hz in both change in power spectrograms and PSDs. Insets in Fig. 8b show a zoomed-in image of the respective change in PSDs to show the difference in these peaks for the three age-groups. Amongst the elderly age-groups, the mean SSVEP change in power was less in the >64 years age-group compared to 50–64 years age-group in both males and females. We regressed the SSVEP power change with age (scatter plot in Fig. 8c bottom row, shown separately for males and females). Change in SSVEP power at 32 Hz decreased significantly with age for both males and females separately (males: $\beta = -0.17$, $R^2 = 0.09$, $p = 0.002$ and females: $\beta = -0.18$, $R^2 = 0.08$, $p = 0.007$) as well as when the data were pooled across genders ($\beta = -0.19$, $R^2 = 0.11$, $p = 1.4 \times 10^{-6}$, regression fit indicated by black line in bottom row of Fig. 8c).

We repeated this analysis for posteromedial group of electrodes and noticed similar results (regression of change in 32 Hz SSVEP power versus age for males: $\beta = -0.16$, $R^2 = 0.11$, $p = 0.0008$, females: $\beta = -0.14$, $R^2 = 0.06$, $p = 0.02$ and for data pooled across gender: $\beta = -0.17$, $R^2 = 0.11$, $p = 1.5 \times 10^{-6}$). We noticed this decrease of 32 Hz SSVEP power with age also in the mean scalp maps for all analyzable electrodes across all subjects in the three age-groups, as depicted in Fig. 8d.

4 Discussion

We tested for age-dependent variation of stimulus-induced change in power and center frequency of narrow-band gamma oscillations in both slow and fast gamma frequency ranges in healthy elderly subjects aged 50–88 years. We observed a decrease in power of both slow and fast gamma oscillations with age, although the decrease in fast gamma was more salient than slow gamma. On the other hand, level of alpha suppression did not change with age in elderly subjects. Finally, center frequency of both gamma rhythms as well as alpha suppression decreased with age in these subjects. As there was no significant change in baseline slow/fast gamma power, eye-position and microsaccade rate across age, we ruled out the possibility that the age-related variations in gamma could be because of such factors. Further, we also studied variation of 32 Hz SSVEP power with age and observed a negative correlation. We also analyzed these results in a cohort of younger subjects (aged 20–48) for comparison.

As noted earlier, Gaetz et al. (2012) had demonstrated a decrease of center frequency (and not power) of fast gamma with age in younger subjects in MEG. We extended these results to elderly subjects, in addition to conclusively demonstrating, for the first time, a decrease of both slow and fast gamma power with age.

4.1 Baseline absolute alpha power and stimulus-induced relative alpha suppression

Previous studies have suggested reduction in baseline alpha power in elderly subjects compared to younger subjects (Babiloni et al., 2006). Also, task-related modulation of alpha power was seen to be reduced in older adults compared to younger subjects (Vaden et al., 2012). Our results were similar to these previous reports: baseline alpha power was significantly higher in younger females versus elderly (Fig. 2b) and showed a decreasing trend with age in males (although not significant, Fig. 2a). Similarly, stimulus-induced alpha suppression was stronger for younger subjects compared to elderly subjects (Fig. 6a). This is notwithstanding the different recording paradigms from previous studies: in our study, baseline alpha was recorded during eyes-open state (as opposed to resting, eyes-closed state in Babiloni and colleagues (2006)) and alpha suppression was measured during passive fixation (as opposed to an active memory task in Vaden and colleagues (2012)). Among the elderly subjects, however, neither baseline alpha power (Fig. 2a and b) nor alpha suppression (Fig. 6a) varied with age. Different results for alpha suppression versus stimulus-induced change in gamma power (which decreased with age) in elderly subjects suggest different biophysical mechanisms of these oscillations.

4.2 Baseline PSD slopes

Some authors have suggested that power-law distribution ($1=f^\beta$, where β is the PSD slope) of brain electrical activity represents broadband scale-free activity of brain that is dependent on behavioral states (He, 2014; He et al., 2010; Podvalny et al., 2015) and cognitive abilities (Sheehan et al., 2018; Voytek et al., 2015). Specifically, Voytek and colleagues had suggested that flattening of PSD slopes might be a hallmark of senile physiological cognitive decline. In our study however, we did not notice any significant correlation between baseline PSD slopes and age in the unipolar reference scheme (as used by Voytek and colleagues), especially for elderly subjects. There are several reasons that could have led to this discrepancy. First, we estimated broadband slopes in the range of 16–44 Hz as opposed to 2–24 Hz (as in Voytek et al.). This is to avoid the contribution of baseline alpha power (8–12 Hz), against which we were testing for slopes (Fig. 2d and Supplementary Fig. 2b). Second, the sample size of Voytek and colleagues was small (11 young and 13 elderly) with a larger proportion of females in the younger group (male:female = 4:7 and 8:5 in young and elderly groups). Because females had steeper slopes than males (Fig. 2c), underrepresentation of females in the elderly group could have led to flatter PSDs in their data. Finally, we found that PSD slopes were correlated with baseline alpha power (which was higher in younger versus elderly), but there was no dependence of slope on age when controlled for baseline alpha power (using partial correlation). Note that a similar correlation of slopes with alpha power in human MEG and EEG as well as monkey ECoG has also been reported by Muthukumaraswamy and Liley (2018).

We note, however, that the PSDs did tend to become flatter with age, albeit at a higher frequency range (>50 Hz; Fig. 2a and b), consistent with the ECoG results of Voytek and colleagues and consistent with the neural noise hypothesis proposed by them. Further, our “spontaneous activity” used for PSD computation was during the fixation task itself, and PSDs were computed using segments of 500 ms, much less than the 2 s segments used by Voytek and colleagues. Consequently, the frequency resolution was 4 times higher in the study of Voytek and colleagues, which could have led to the identification of small changes in slopes better than ours. Longer stimulus-free epochs (at least 2 s or more), preferentially in both eyes closed and eyes open conditions are required to test whether the flattening of PSD slope occurs at lower frequencies as well.

4.3 Possible confounds from ocular factors

Broadband induced gamma responses have been proposed to be correlated with occurrence of microsaccades (Yuval-Greenberg et al., 2008). However, in our previous study, we did not note any effect of microsaccades on orientation tuning of narrow-band slow and fast gamma oscillations in macaques (Murty et al., 2018). Consistently, we did not find any effect of microsaccades on age-dependent decrease of slow and fast gamma power in this study.

It is possible that retinal illuminance is reduced due to senile pupillary miosis, which is indirectly reflected in the reduced pupillary reactivity to stimulus presentation across age (Fig. 7c). Other abnormalities of peripheral visual system like age-related increase in density of crystalline lens, age-related macular degeneration, etc. could have had affected our results (Owsley, 2011). The subjects did not undergo a thorough ophthalmic examination due to

time limitations. However, we argue that the results presented here are likely due to neurophysiological effects of aging on two grounds. First, in addition to a reduction in gamma power, there is a reduction in gamma center frequency with age, which is harder to explain based on the abnormalities listed above. Second, slow/fast gamma power was not dependent on pupillary reactivity to stimulus (Fig. 7d). Nonetheless, we observed that the percentage of variance in the gamma power/frequency or SSVEP power explained by age is very small. Maximum R^2 among all cases was 0.11 (for decrease in SSVEP power across age in posteromedial electrodes). Hence, we recognize that age is one of the many possible factors that influence gamma power/frequency and do not completely rule out the possibility that any hidden physiological variables could have had contributed to this variance.

4.4 Possible mechanisms of age-related reductions in gamma frequency and change in power

It is suggested that gamma rhythms are generated by excitatory/inhibitory interactions in the brain (Buzsáki and Wang, 2012). Such interactions could be influenced by many factors, such as axonal length/diameter (affecting axonal conduction velocity, see Buzsáki et al., 2013), myelination (Buzsáki et al., 2013), gene expression of synaptic proteins related to GABAergic mechanisms, etc. How such structural and microscopic differences and maturation across aging influence gamma recorded over scalp is unknown. Previous studies in MEG had reported significant positive correlations between (fast) gamma frequency and cortical thickness as well as volume of cuneus (Gaetz et al., 2012) and thickness of pericalcarine area (Muthukumaraswamy et al., 2010), measured through structural MRI. Further, (fast) gamma peak frequency has been positively correlated with brain GABA levels (Edden et al., 2009; Muthukumaraswamy et al., 2009). However, such results failed replication (Cousijn et al., 2014) and have been shown to be confounded by age (Robson et al., 2015) which stands as a common factor that influences both macroscopic structure as well as synaptic function. For example, age-related decreases in cortical volume, thickness and/or surface area were observed in various regions of the brain like precuneus, cuneus, lingual, pericalcarine and lateral occipital areas of the occipital cortex (Lemaitre et al., 2012; Salat et al., 2004; van Pelt et al., 2018). Similarly, synaptic expression of certain proteins related to GABAergic transmission has been shown to be influenced by age (Pinto et al., 2010).

Many non-neural factors have also been postulated to influence gamma power recorded at the sensor and scalp level, such as the distance between active cortex and electrode (Butler et al., 2019). These authors noticed a strong negative correlation of change in gamma power with skull thickness and showed that gamma peak frequency is more immune to such morphological factors. Further, Sumner et al. (2018) observed that gamma activity could be influenced by circulating gonadal hormones. They suggested that such influences cause differences in gamma activity across menstrual cycle. While we did not explicitly ask for menstrual history from our female volunteers (which is a limitation of our study), most of them were aged above 55 years and hence were in the post-menopausal period of life. Moreover, our results did not differ when we considered male and female participants separately (Figs. 4, 6 and 8). Hence, we speculate that age might have had influenced gamma activity in our study independent of sex-hormonal factors. However, as described

above, there could be a myriad of mechanisms through which age could have had influenced gamma activity in our study, which are difficult to be delineated and hence remain elusive and unanswered.

5 Conclusion

Our study throws light on various features of baseline spectra (like baseline alpha power and its relation to PSD slopes) and spectral responses to Cartesian gratings (alpha suppression, slow and fast gamma) in a large cohort of healthy elderly. Our study could thus act as normative for future gamma and SSVEP studies in the elderly age-group. Further, based on observations in previous rodent studies (Iaccarino et al., 2016; for example, Verret et al., 2012) as described before, some authors have suggested a causative role of (fast) gamma disruption in neurodegenerative disorders of aging such as AD (Palop and Mucke, 2016). Alternatively, our results suggest that gamma and SSVEPs suffer reduction in power with age even in the absence of cognitive decline. Interestingly, such reduction in gamma power with aging has also been observed in motor areas (Gaetz et al., 2020), suggesting that this could be a generic phenomenon across different brain areas. These studies taken together, decrease in gamma/SSVEP power may represent a continuum of healthy aging – preclinical cognitive decline – dementia spectrum and may act as a harbinger to senile or pathological cognitive decline, a hypothesis that needs to be tested in future studies.

Supplementary Material

Refer to Web version on PubMed Central for supplementary material.

Funding

This work was supported by Wellcome Trust/DBT India Alliance (Intermediate fellowship 500145/Z/09/Z and Senior fellowship IA/S/18/2/504003 to SR), Tata Trusts Grant and DBT-IISc Partnership Programme.

Abbreviations

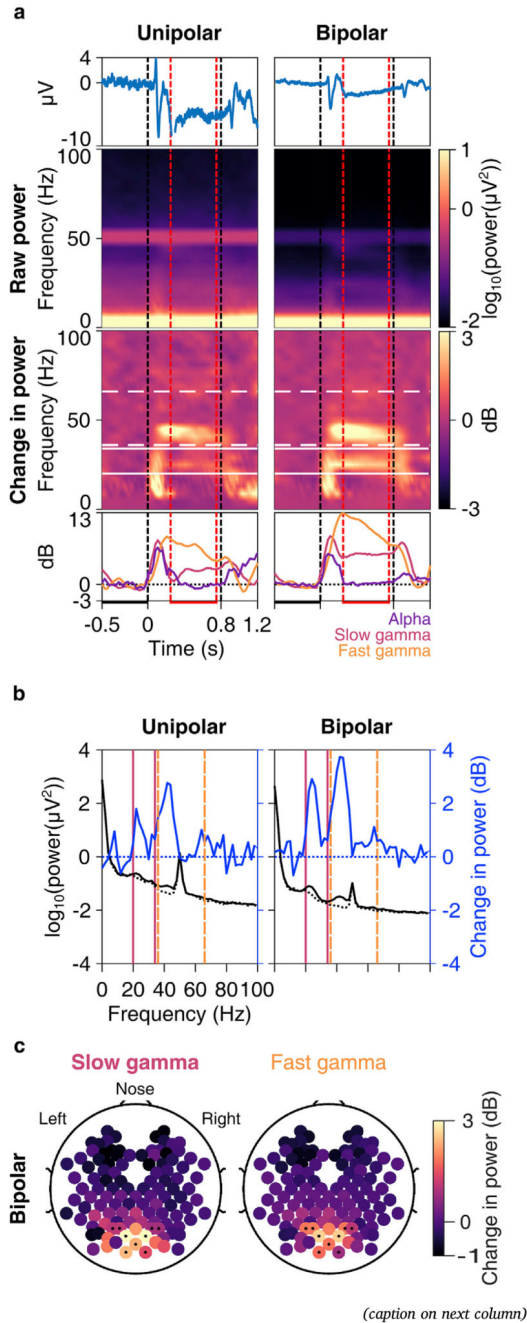
AD	Alzheimer's disease
CV	coefficient of variation
GABA	gamma-aminobutyric acid
LFP	local field potentials
PSD	power spectral density
SD	standard deviation
SEM	standard error of the mean
SF	spatial frequency
SSVEP	steady-state visual evoked potentials

References

- An K, Ikeda T, Yoshimura Y, Hasegawa C, Saito DN, Kumazaki H, Hirosawa T, Minabe Y, Kikuchi M. Altered gamma oscillations during motor control in children with autism spectrum disorder. *J Neurosci*. 2018; 38:7878–7886. DOI: 10.1523/JNEUROSCI.1229-18.2018 [PubMed: 30104338]
- Babiloni C, Binetti G, Cassarino A, Forno GD, Percio CD, Ferreri F, Ferri R, Frisoni G, Galderisi S, Hirata K, Lanuzza B, et al. Sources of cortical rhythms in adults during physiological aging: a multicentric EEG study. *Hum Brain Mapp*. 2006; 27:162–172. DOI: 10.1002/hbm.20175 [PubMed: 16108018]
- Butler R, Bernier PM, Mierzwinski GW, Descoteaux M, Gilbert G, Whittingstall K. Cortical distance, not cancellation, dominates inter-subject EEG gamma rhythm amplitude. *Neuroimage*. 2019; 192:156–165. DOI: 10.1016/j.neuroimage.2019.03.010 [PubMed: 30858117]
- Buzsáki G, Logothetis N, Singer W. Scaling brain size, keeping timing: evolutionary preservation of brain rhythms. *Neuron*. 2013; 80:751–764. DOI: 10.1016/j.neuron.2013.10.002 [PubMed: 24183025]
- Buzsáki G, Wang X-J. Mechanisms of gamma oscillations. *Annu Rev Neurosci*. 2012; 35:203–225. DOI: 10.1146/annurev-neuro-062111-150444 [PubMed: 22443509]
- Cardin JA, Carlen M, Meletis K, Knoblich U, Zhang F, Deisseroth K, Tsai L-H, Moore CI. Driving fast-spiking cells induces gamma rhythm and controls sensory responses. *Nature*. 2009; 459:663–667. DOI: 10.1038/nature08002 [PubMed: 19396156]
- Chalk M, Herrero JL, Gieselmann MA, Delicato LS, Gotthardt S, Thiele A. Attention reduces stimulus-driven gamma frequency oscillations and spike field coherence in V1. *Neuron*. 2010; 66:114–125. DOI: 10.1016/j.neuron.2010.03.013 [PubMed: 20399733]
- Colgin LL, Denninger T, Fyhn M, Hafting T, Bonnevie T, Jensen O, Moser M-B, Moser EI. Frequency of gamma oscillations routes flow of information in the hippocampus. *Nature*. 2009; 462:353–357. DOI: 10.1038/nature08573 [PubMed: 19924214]
- Cousijn H, Haegens S, Wallis G, Near J, Stokes MG, Harrison PJ, Nobre AC. Resting GABA and glutamate concentrations do not predict visual gamma frequency or amplitude. *Proc Natl Acad Sci Unit States Am*. 2014; doi: 10.1073/pnas.1321072111
- Delorme A, Makeig S. EEGLAB: an open source toolbox for analysis of single-trial EEG dynamics including independent component analysis. *J Neurosci Methods*. 2004; 134:9–21. DOI: 10.1016/j.jneumeth.2003.10.009 [PubMed: 15102499]
- Edden RAE, Muthukumaraswamy SD, Freeman TCA, Singh KD. Orientation discrimination performance is predicted by GABA concentration and gamma oscillation frequency in human primary visual cortex. *J Neurosci*. 2009; 29:15721–15726. DOI: 10.1523/JNEUROSCI.4426-09.2009 [PubMed: 20016087]
- Engbert, R. Microsaccades: a microcosm for research on oculomotor control, attention, and visual perception. *Progress in Brain Research, Visual Perception*. Martinez-Conde, S, Macknik, SL, Martinez, LM, Alonso, J-M, Tse, PU, editors. Elsevier; 2006. 177–192.
- Gaetz W, Rhodes E, Bloy L, Blaskey L, Jackel CR, Brodtkin ES, Waldman A, Embick D, Hall S, Roberts TPL. Evaluating motor cortical oscillations and age-related change in autism spectrum disorder. *Neuroimage*. 2020; 207doi: 10.1016/j.neuroimage.2019.116349
- Gaetz W, Roberts TPL, Singh KD, Muthukumaraswamy SD. Functional and structural correlates of the aging brain: relating visual cortex (V1) gamma band responses to age-related structural change. *Hum Brain Mapp*. 2020; 33:2035–2046. DOI: 10.1002/hbm.21339
- Gray CM, Koehnig P, Engel AK, Singer W. Oscillatory responses in cat visual cortex exhibit inter-columnar synchronization which reflects global stimulus properties. *Nature*. 1989; 338:334–337. DOI: 10.1038/338334a0 [PubMed: 2922061]
- Gregoriou GG, Gotts SJ, Zhou H, Desimone R. High-frequency, long-range coupling between prefrontal and visual cortex during attention. *Science*. 2009; 324:1207–1210. DOI: 10.1126/science.1171402 [PubMed: 19478185]
- He BJ. Scale-free brain activity: past, present, and future. *Trends Cognit Sci*. 2014; 18:480–487. DOI: 10.1016/j.tics.2014.04.003 [PubMed: 24788139]

- He BJ, Zempel JM, Snyder AZ, Raichle ME. The temporal structures and functional significance of scale-free brain activity. *Neuron*. 2010; 66:353–369. DOI: 10.1016/j.neuron.2010.04.020 [PubMed: 20471349]
- Hirano Y, Oribe N, Kanba S, Onitsuka T, Nestor PG, Spencer KM. Spontaneous gamma activity in schizophrenia. *JAMA Psychiatr*. 2015; 72:813–821. DOI: 10.1001/jamapsychiatry.2014.2642
- Iaccarino HF, Singer AC, Martorell AJ, Rudenko A, Gao F, Gillingham TZ, Mathys H, Seo J, Kritskiy O, Abdurrob F, Adaikkan C, et al. Gamma frequency entrainment attenuates amyloid load and modifies microglia. *Nature*. 2016; 540:230. doi: 10.1038/nature20587 [PubMed: 27929004]
- Ishii R, Canuet L, Aoki Y, Hata M, Iwase M, Ikeda S, Nishida K, Ikeda M. Healthy and pathological brain aging: from the perspective of oscillations, functional connectivity, and signal complexity. *Neuropsychobiology*. 2017; 75:151–161. DOI: 10.1159/000486870 [PubMed: 29466802]
- Jia X, Tanabe S, Kohn A. Gamma and the coordination of spiking activity in early visual cortex. *Neuron*. 2013; 77:762–774. DOI: 10.1016/j.neuron.2012.12.036 [PubMed: 23439127]
- Kropotov, JD. Alpha rhythms Functional Neuromarkers for Psychiatry. Elsevier; 2016. 89–105.
- Lemaitre H, Goldman AL, Sambataro F, Verchinski BA, Meyer-Lindenberg A, Weinberger DR, Mattay VS. Normal age-related brain morphometric changes: nonuniformity across cortical thickness, surface area and gray matter volume? *Neurobiol Aging*. 2012; 33:617.e1–617.e9. DOI: 10.1016/j.neurobiolaging.2010.07.013
- Mably AJ, Colgin LL. Gamma oscillations in cognitive disorders. *Curr Opin Neurobiol Syst Neurosci*. 2018; 52:182–187. DOI: 10.1016/j.conb.2018.07.009
- Mitra, P, Bokil, H. Observed Brain Dynamics. Oxford University Press; Oxford New York: 2008.
- Murty DVPS, Shirhatti V, Ravishankar P, Ray S. Large visual stimuli induce two distinct gamma oscillations in primate visual cortex. *J Neurosci*. 2018; 38:2730–2744. DOI: 10.1523/JNEUROSCI.2270-17.2017 [PubMed: 29440388]
- Muthukumaraswamy SD, Edden RAE, Jones DK, Swettenham JB, Singh KD. Resting GABA concentration predicts peak gamma frequency and fMRI amplitude in response to visual stimulation in humans. *Proc Natl Acad Sci Unit States Am*. 2009; 106:8356–8361. DOI: 10.1073/pnas.0900728106
- Muthukumaraswamy SD, Liley DTJ. 1/f electrophysiological spectra in resting and drug-induced states can be explained by the dynamics of multiple oscillatory relaxation processes. *Neuroimage*. 2018; 179:582–595. DOI: 10.1016/j.neuroimage.2018.06.068 [PubMed: 29959047]
- Muthukumaraswamy SD, Singh KD, Swettenham JB, Jones DK. Visual gamma oscillations and evoked responses: variability, repeatability and structural MRI correlates. *Neuroimage*. 2010; 49:3349–3357. DOI: 10.1016/j.neuroimage.2009.11.045 [PubMed: 19944770]
- Owsley C. Aging and vision. *Vis Res*. 2011; 51:1610–1622. DOI: 10.1016/j.visres.2010.10.020 [PubMed: 20974168]
- Palop JJ, Mucke L. Network abnormalities and interneuron dysfunction in Alzheimer disease. *Nat Rev Neurosci*. 2016; 17:777–792. DOI: 10.1038/nrn.2016.141 [PubMed: 27829687]
- Pantazis D, Fang M, Qin S, Mohsenzadeh Y, Li Q, Cichy RM. Decoding the orientation of contrast edges from MEG evoked and induced responses. *NeuroImage, New advances in encoding and decoding of brain signals*. 2018; 180:267–279. DOI: 10.1016/j.neuroimage.2017.07.022
- Pesaran B, Pezaris JS, Sahani M, Mitra PP, Andersen RA. Temporal structure in neuronal activity during working memory in macaque parietal cortex. *Nat Neurosci*. 2002; 5:805–811. DOI: 10.1038/nn890 [PubMed: 12134152]
- Pinto JGA, Hornby KR, Jones DG, Murphy KM. Developmental changes in GABAergic mechanisms in human visual cortex across the lifespan. *Front Cell Neurosci*. 2010; 4:doi: 10.3389/fncel.2010.00016
- Podvalny E, Noy N, Harel M, Bickel S, Chechik G, Schroeder CE, Mehta AD, Tsodyks M, Malach R. A unifying principle underlying the extracellular field potential spectral responses in the human cortex. *J Neurophysiol*. 2015; 114:505–519. DOI: 10.1152/jn.00943.2014 [PubMed: 25855698]
- Ray S, Maunsell JHR. Do gamma oscillations play a role in cerebral cortex? *Trends Cognit Sci*. 2015; 19:78–85. DOI: 10.1016/j.tics.2014.12.002 [PubMed: 25555444]
- Robson SE, Muthukumaraswamy SD, Evans CJ, Shaw A, Brealy J, Davis B, McNamara G, Perry G, Singh KD. Structural and neurochemical correlates of individual differences in gamma frequency

- oscillations in human visual cortex. *J Anat.* 2015; 227:409–417. DOI: 10.1111/joa.12339 [PubMed: 26352409]
- Sahoo B, Pathak A, Deco G, Banerjee A, Roy D. Lifespan associated changes in global patterns of coherent communication. *bioRxiv.* 2020; doi: 10.1101/504589
- Salat DH, Buckner RL, Snyder AZ, Greve DN, Desikan RSR, Busa E, Morris JC, Dale AM, Fischl B. Thinning of the cerebral cortex in aging. *Cerebr Cortex.* 2004; 14:721–730. DOI: 10.1093/cercor/bhh032
- Salelkar S, Ray S. Interaction between steady-state visually evoked potentials at nearby flicker frequencies. *Sci Rep.* 2020; 10:1–16. DOI: 10.1038/s41598-020-62180-y [PubMed: 31913322]
- Sheehan TC, Sreekumar V, Inati SK, Zaghoul KA. Signal complexity of human intracranial EEG tracks successful associative-memory formation across individuals. *J Neurosci.* 2018; 38:1744–1755. DOI: 10.1523/JNEUROSCI.2389-17.2017 [PubMed: 29330327]
- Shirhatti V, Borthakur A, Ray S. Effect of reference scheme on power and phase of the local field potential. *Neural Comput.* 2016; 28:882–913. DOI: 10.1162/NECO_a_00827 [PubMed: 26942748]
- Sohal VS, Zhang F, Yizhar O, Deisseroth K. Parvalbumin neurons and gamma rhythms enhance cortical circuit performance. *Nature.* 2009; 459:698–702. DOI: 10.1038/nature07991 [PubMed: 19396159]
- Sumner RL, McMillan RL, Shaw AD, Singh KD, Sundram F, Muthukumaraswamy SD. Peak visual gamma frequency is modified across the healthy menstrual cycle. *Hum Brain Mapp.* 2018; 39:3187–3202. DOI: 10.1002/hbm.24069 [PubMed: 29665216]
- Tada M, Nagai T, Kirihara K, Koike S, Suga M, Araki T, Kobayashi T, Kasai K. Differential alterations of auditory gamma oscillatory responses between preonset high-risk individuals and first-episode schizophrenia. *Cerebr Cortex.* 2014; doi: 10.1093/cercor/bhu278bhu278
- Uhlhaas PJ, Singer W. What do disturbances in neural synchrony tell us about autism? *Biol Psychiatr Mech Circuit Dysfunct Neurodev Disorders.* 2007; 62:190–191. DOI: 10.1016/j.biopsych.2007.05.023
- Vaden RJ, Hutcheson NL, McCollum LA, Kentros J, Visscher KM. Older adults, unlike younger adults, do not modulate alpha power to suppress irrelevant information. *Neuroimage.* 2012; 63:1127–1133. DOI: 10.1016/j.neuroimage.2012.07.050 [PubMed: 22885248]
- van Pelt S, Shumskaya E, Fries P. Cortical volume and sex influence visual gamma. *Neuroimage.* 2018; 178:702–712. DOI: 10.1016/j.neuroimage.2018.06.005 [PubMed: 29883733]
- Veit J, Hakim R, Jadi MP, Sejnowski TJ, Adesnik H. Cortical gamma band synchronization through somatostatin interneurons. *Nat Neurosci.* 2017; 20:951–959. DOI: 10.1038/nn.4562 [PubMed: 28481348]
- Verret L, Mann EO, Hang GB, Barth AMI, Cobos I, Ho K, Devidze N, Masliah E, Kreitzer AC, Mody I, Mucke L, et al. Inhibitory interneuron deficit links altered network activity and cognitive dysfunction in alzheimer model. *Cell.* 2012; 149:708–721. DOI: 10.1016/j.cell.2012.02.046 [PubMed: 22541439]
- Voytek B, Kramer MA, Case J, Lepage KQ, Tempesta ZR, Knight RT, Gazzaley A. Age-related changes in 1/f neural electrophysiological noise. *J Neurosci.* 2015; 35:13257–13265. DOI: 10.1523/JNEUROSCI.2332-14.2015 [PubMed: 26400953]
- Whitham EM, Lewis T, Pope KJ, Fitzgibbon SP, Clark CR, Loveless S, DeLosAngeles D, Wallace AK, Broberg M, Willoughby JO. Thinking activates EMG in scalp electrical recordings. *Clin Neurophysiol.* 2008; 119:1166–1175. DOI: 10.1016/j.clinph.2008.01.024 [PubMed: 18329954]
- Wilson TW, Rojas DC, Reite ML, Teale PD, Rogers SJ. Children and adolescents with autism exhibit reduced MEG steady-state gamma responses. *Biol Psychiatr Mech Circuit Dysfunct Neurodev Disorders.* 2007; 62:192–197. DOI: 10.1016/j.biopsych.2006.07.002
- Yuval-Greenberg S, Tomer O, Keren AS, Nelken I, Deouell LY. Transient induced gamma-band response in EEG as a manifestation of miniature saccades. *Neuron.* 2008; 58:429–441. DOI: 10.1016/j.neuron.2008.03.027 [PubMed: 18466752]



(caption on next column)

Fig. 1. Slow and fast gamma in an example elderly subject.

a) Trial-averaged EEG trace (1st row, blue); time–frequency spectrograms of raw power (2nd row) and change in power from baseline (3rd row); and change in power with time (4th row) in alpha (8–12 Hz, violet), slow (20–34 Hz, pink) and fast gamma (36–66 Hz, orange) bands averaged across 10 unipolar (left column) and 9 bipolar (right column) electrodes. Vertical dashed lines represent actual stimulus duration (0–0.8 s, black) and period used for analysis within stimulus duration (0.25–0.75 s, red). Horizontal lines represent baseline (-0.5–0 s, black) and stimulus (0.25–0.75 s, red) analysis periods. White lines in spectrograms

represent slow (solid) and fast (dashed) gamma frequency ranges. b) Right ordinate shows raw power spectral densities (PSDs, black traces) vs frequency in baseline (dotted) and stimulus (solid) periods averaged across 10 unipolar electrodes (left column) and 9 bipolar (right column) electrodes; left ordinate shows the same for change in PSD (in dB, solid blue trace) in stimulus period from baseline. Solid pink lines and dashed orange lines represent slow and fast gamma bands respectively. c) Scalp maps showing 112 bipolar electrodes (represented as disks). Color of each disk represents change in slow (left) and fast (right) gamma power. 9 electrodes used in 1a and 1b (right column) are marked with dots.

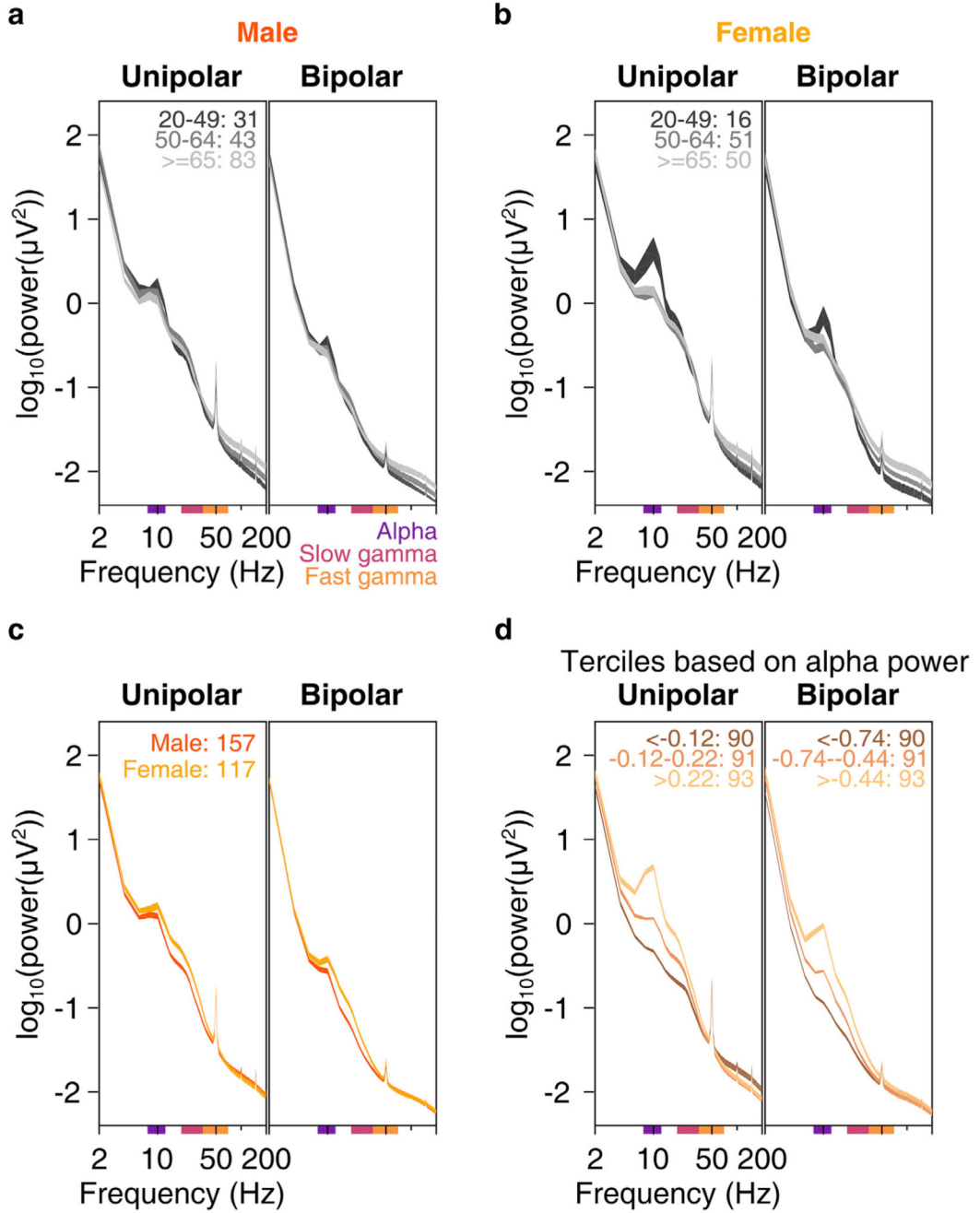


Fig. 2. Baseline PSDs, slopes and alpha power.

Baseline PSDs (averaged across 10 unipolar or 9 bipolar electrodes) for three age-groups on a log-log scale for unipolar (left) and bipolar (right) reference, plotted for males (2a) and females (2b). Thickness of traces indicate SEM across subjects. Age-group limits and the number of subjects in the respective age-groups are indicated on the left plot. c) Same as in 2a and 2b, but for males and females, pooled across all age-groups. d) Mean baseline PSDs for three ranges of baseline absolute alpha power (8–12 Hz, power ranges for respective traces indicated on the plots) pooled across all age-groups. Thickness of traces and numbers

indicate SEM across subjects and number of subjects in respective alpha power ranges. Colored bars on the abscissa indicate alpha (8–12 Hz, violet), slow (20–34 Hz, pink) and fast gamma (36–66 Hz, orange) frequency bands.

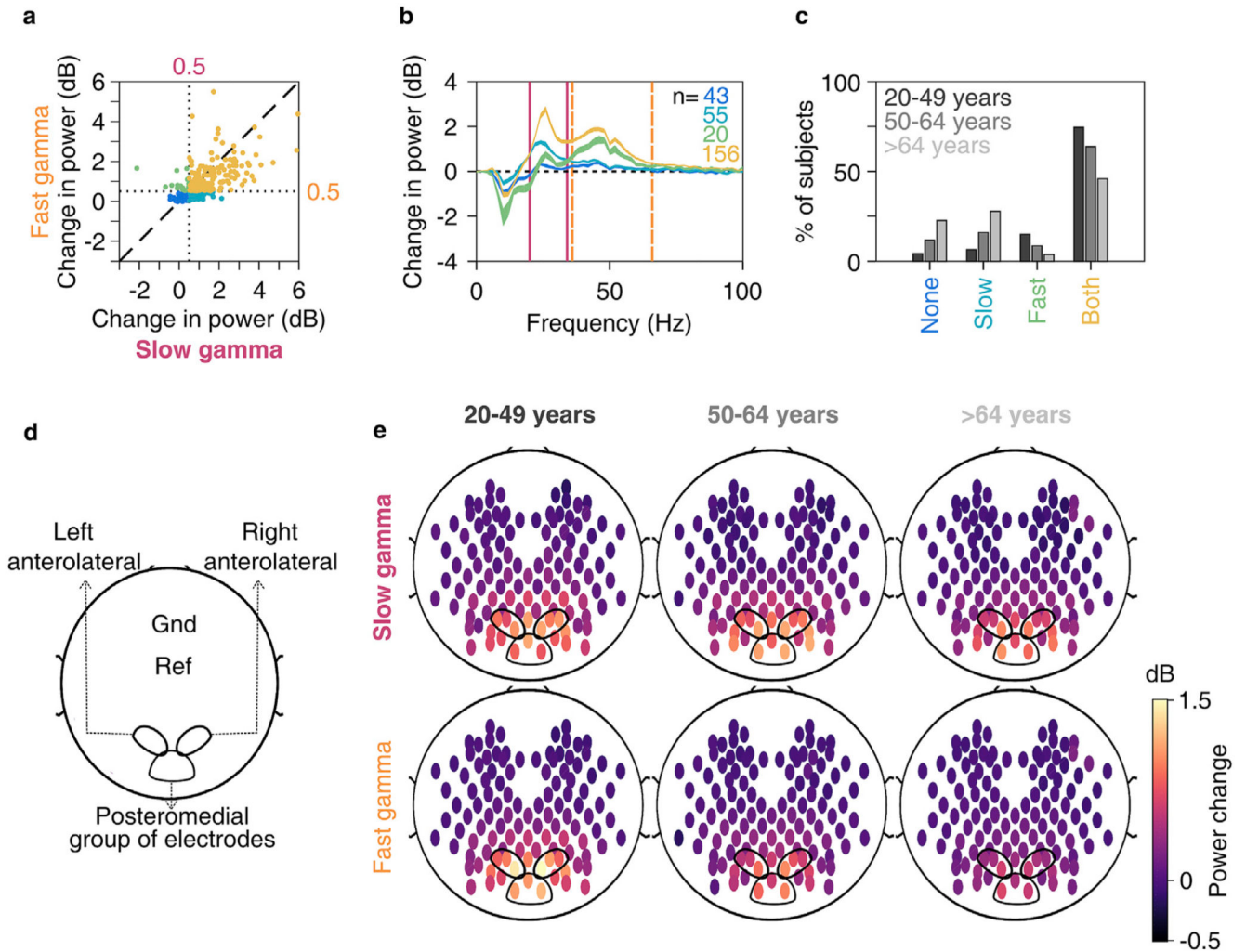


Fig. 3. Slow and fast gamma in younger and elderly subjects.

a) Scatter plot showing change in slow (abscissa) and fast (ordinate) gamma power. Dotted lines represent 0.5 dB threshold. Points represent subjects with no gamma (dark blue), only slow gamma (light blue), only fast gamma (green) and both gamma rhythms (yellow) with change in power above 0.5 dB threshold. b) Change in PSDs vs frequency averaged across subjects (numbers denoted by n) as categorized in 3a. Thickness of traces indicate SEM. Solid pink and dashed lines represent slow and fast gamma ranges respectively. c) Bar plot showing percentage of subjects in three age-groups (marked by respective colors) categorized as in 3a. d) Schematic showing placements of left and right anterolateral and posteromedial group of bipolar electrodes used for analysis on the scalp, as well as ground (Gnd) and online reference (Ref) electrodes. e) Average scalp maps of 112 bipolar electrodes (disks) for three age-groups for slow (top row) and fast (bottom row) gamma. Color of disks represents change in respective gamma power. Electrode groups represented as in 3d.

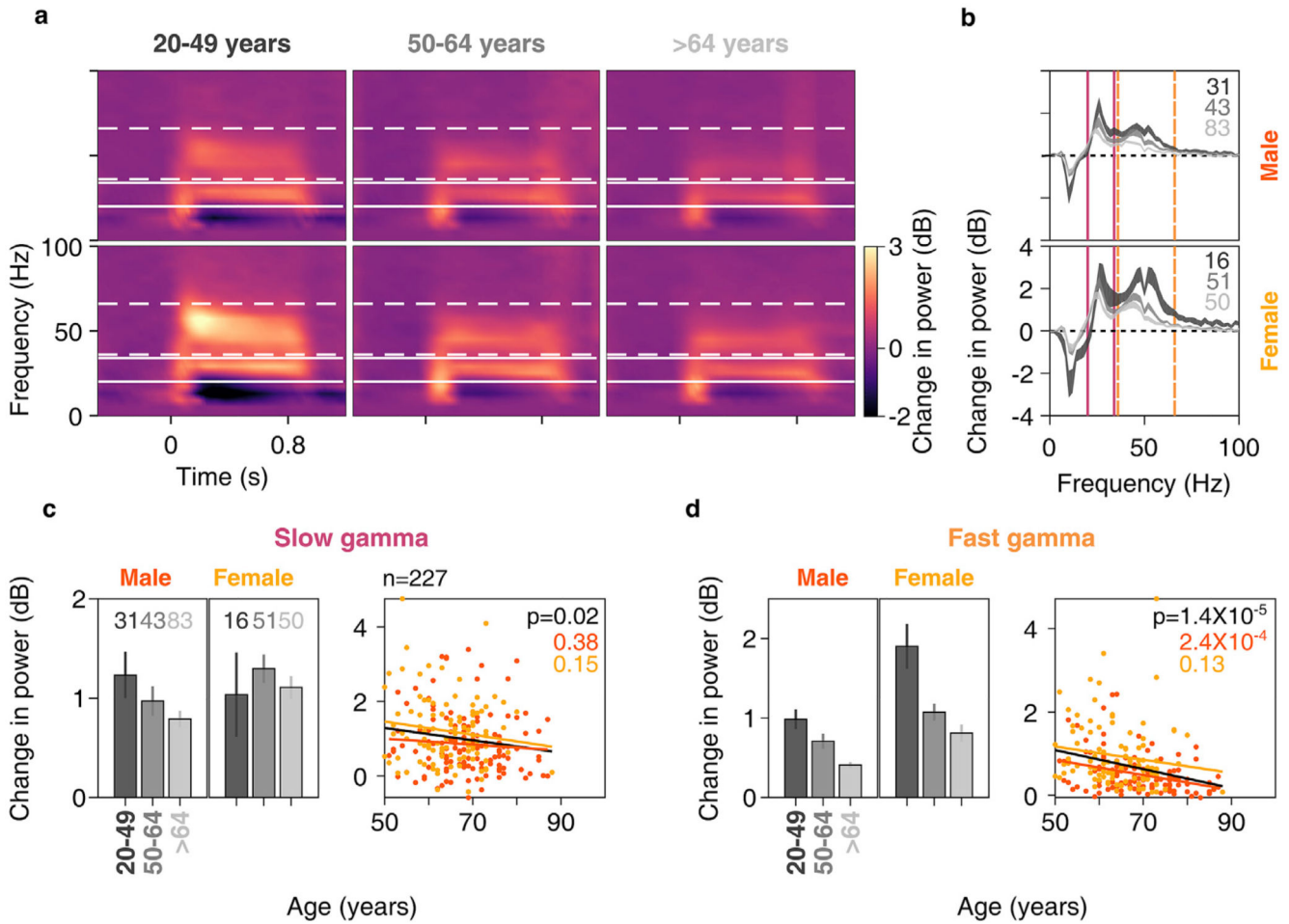


Fig. 4. Change in gamma power vs age for anterolateral group of electrodes.

Mean time-frequency change in power spectrograms (4a) and change in power spectra vs frequency (4b) for three age-groups separately for males (top row) and females (bottom row). Thickness of traces and numbers in 4b indicate SEM and number of subjects respectively. Solid and dashed lines indicate slow and fast gamma frequency ranges respectively. c) Left column: bar plots showing mean change in slow gamma power for three age-groups separately for males and females. Number of subjects for respective age-groups are indicated on top. Error bars indicate SEM. Right column: scatter plot for change in slow gamma power vs age for all elderly subjects (>49 years age-group, $n = 227$), plotted separately for males (in orange) and females (in yellow). Orange, yellow and black solid lines indicate regression fits for males, females and data pooled across gender respectively. p-values of the regression fits are indicated in respective colors. d) Same as in 4c but for fast gamma.

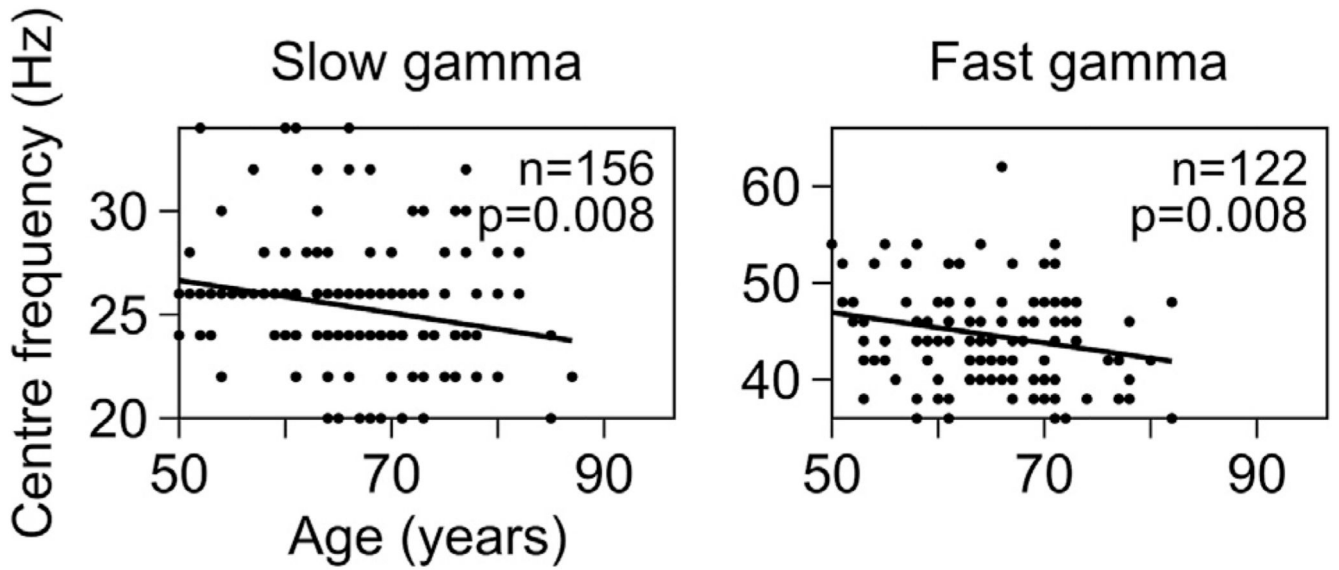


Fig. 5. Center frequency of slow and fast gamma vs age for elderly subjects for anterolateral group of electrodes.

Scatter plots showing center frequency vs age for slow and fast gamma, for anterolateral electrodes, for those subjects who have change in power in respective gamma range above 0.5 dB (numbers indicated on the plots). Solid lines indicate regression fits for center frequency vs age. p-values for these fits are as indicated.

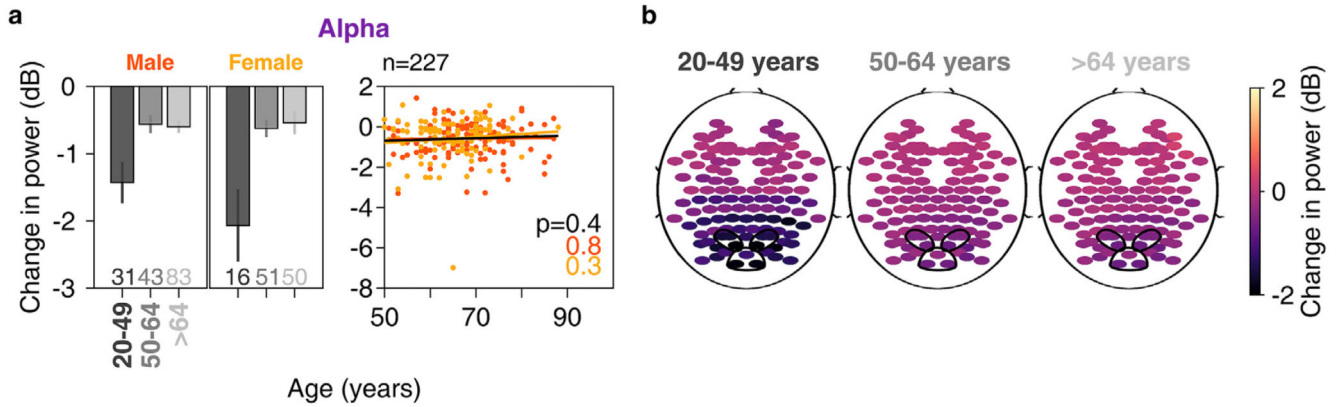


Fig. 6. Change in alpha power vs age.

a) Left column: bar plots showing mean change in alpha power across anterolateral group of electrodes for three age-groups separately for males and females. Number of subjects for respective age-groups are indicated at bottom. Right column: scatter plot for change in alpha power vs age for all elderly subjects (>49 years age-group, $n = 227$), plotted separately for males (in orange) and females (in yellow). Same format as in Fig. 4c b) Scalp maps for 112 electrodes (disks) averaged across all subjects separately for three age-groups. Color indicates change in alpha power for each electrode, same format as in Fig. 3e.

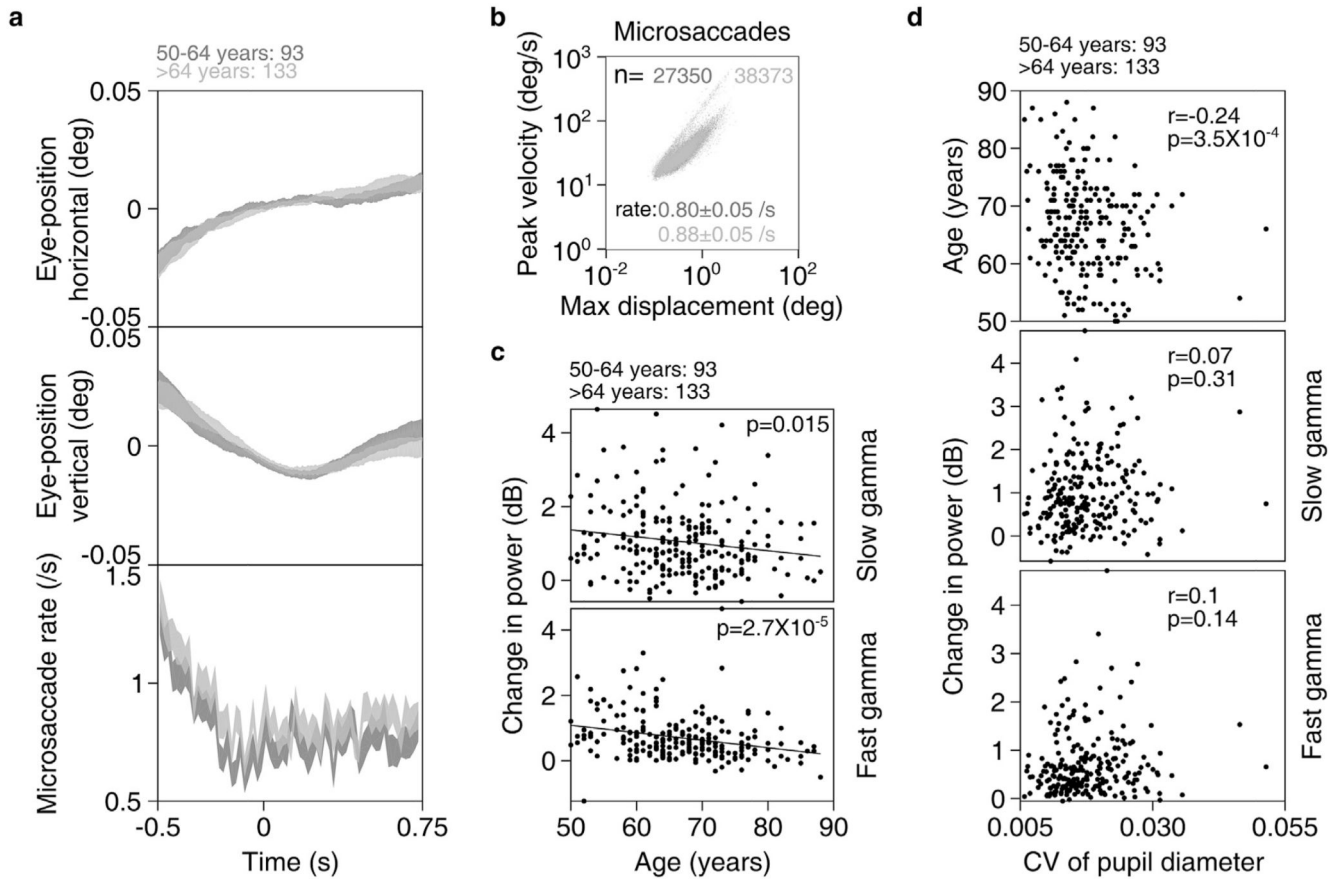


Fig. 7. Eye position, microsaccades and pupillary reactivity across age for elderly subjects.

a) Eye-position in horizontal (top row) and vertical (middle row) directions; and histogram showing microsaccade rate (bottom row) vs time (-0.5–0.75 s of stimulus onset) for elderly subjects ($n = 226$). Number of subjects in each age-group is indicated on top. Thickness indicates SEM. b) Main sequence showing peak velocity and maximum displacement of all microsaccades (number indicated by n) extracted for both elderly age-groups. Average microsaccade rate (mean \pm SEM) across all subjects for each elderly age-group is also indicated. c) Scatter plot showing change in power vs age for slow (top row) and fast (bottom row) gamma for all elderly subjects with analyzable data after removal of trials containing microsaccades. Solid lines indicate regression fits. Numbers of subjects with analyzable data in each age-group is indicated on top. d) Scatter plots for coefficient of variation (CV) of pupil diameter vs age (top row), change in slow (middle row) and fast (bottom row) gamma power. Pearson correlation coefficients (r) and p -values are also indicated.

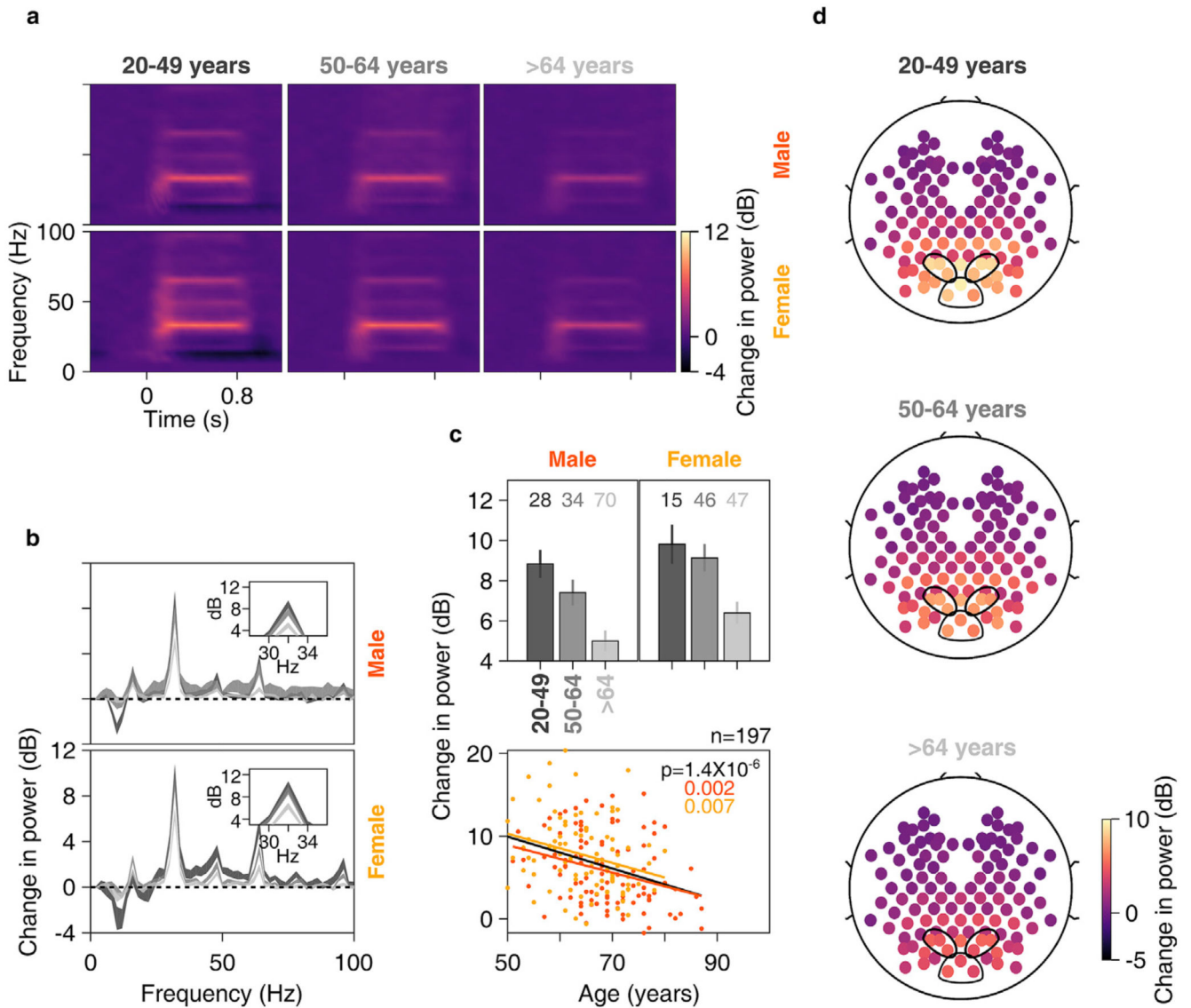


Fig. 8. Change in SSVEP power vs age for anterolateral group of electrodes.

Time-frequency change in power spectrograms (8a) and change in power spectra vs frequency (8b) for three age-groups separately for males (top row) and females (bottom row). Thickness of traces in 8b indicates SEM. Insets in 8b display zoomed-in images of respective main plots, showing clear SSVEP peaks at 32 Hz. c) Top row: bar plots showing mean change in SSVEP power for three age-groups separately for males and females; numbers of subjects in each age-group is indicated on top. Error bars indicate SEM. Bottom row: scatter plot for change in SSVEP power vs age for all elderly subjects (>49 years age-group, $n = 197$), plotted separately for males (in orange) and females (in yellow). Orange, yellow and black solid lines indicate regression fits for males, females and data pooled across gender respectively. p-values of the regression fits are indicated in respective colors.

d) Scalp maps for 112 electrodes (disks) averaged across all subjects separately for three age-groups. Color indicates change in SSVEP power at 32 Hz for each electrode.